PHOTOCATALYTIC DEGRADATION OF LOW DENSITY POLYETHYLENE (LDPE) FILMS USING TITANIA NANOTUBES

A thesis submitted in partial fulfillment of the requirements for the degree

of

Master of Science

in

Environmental Science

by

Saba Sadaqat Ali

(NUST-01261071MSCEE65212F)

Institute of Environmental Sciences & Engineering (IESE)

School of Civil and Environmental Engineering (SCEE)
National University Of Sciences and Technology (NUST)

Islamabad, Pakistan
(2015)

APPROVAL SHEET

"PHOTOCATALYTIC DEGRADATION OF LOW DENSITY POLYETHYLENE
(LDPE) FILMS USING TITANIA NANAOTUBES"

It is certified that the contents and form of the thesis entitled

submitted by

Saba Sadaqat Ali

Has been found satisfactory for the requirements of the degree of Master of Science in

Environmental Science.

Supervisor: _____
Dr. Ishtiaq A. Qazi
Professor & Associate Dean
IESE, SCEE, NUST

Member: _____
Dr. Muhammad Arshad
Assistant Professor
IESE, SCEE, NUST

Member: _____
Dr. Zahiruddin Khan
Associate Professor
IESE, SCEE, NUST

Member:_____
Dr. Thomas C. Voice
Professor,
MSU, USA

بسم الله الرحمن الرحيم

This thesis is dedicated to my parents

for their love and dedicated partnership for success in my

life and my brother Muhammad Faisal for his affection and

moral support throughout my academic career

ACKNOWLEDGEMENTS

Abstract

Polyethylene (PE) waste disposal is one of the critical issues of the modern lifestyle which poses serious threat to human health and environment. The present study was designed to investigate the photocatalytic degradation of LDPE films using titania nanotubes (TNTs) under UV and visible light while carrying out a comparative study using titania nanoparticles (TNPs) under the same experimental conditions. Dye sensitization of the nanostructures was done to enhance their catalytic efficiency. TNPs and TNTs were prepared from general purpose TiO_2 by liquid impregnation and hydrothermal methods respectively. LDPE films with or without the nanomaterial were prepared by dissolving LDPE pellets in cyclohexane and evaporating the solvent in Petri plates. These LDPE films were then kept under UV and visible light separately for upto 45 days. The degradation of pure and composite LDPE films was measured in terms of photo induced weight loss and was confirmed by FTIR, SEM, surface roughness and tensile strength testing. The results show that the dye sensitized titania nanotubes were very effective in degrading the LDPE films under visible light, indicating that plastic bags containing such material can be prepared that would be degradable in the open environment.

Table of Contents

List of Figures

List of Tables

List of Abbreviations

ASTM	American Society for Testing and Materials
BET	Brunauer Edward Teller
BG	Brilliant Green
EDS	Energy Dispersive Spectroscopy
eV	Electron Volt
FTIR	Fourier Transform Infrared Spectroscopy
GPR	General Purpose Reagent
HCl	Hydrochloric Acid
PET	Polyethylene Terephthalate
PVC	Polyvinyl Chloride
SC	Semiconductor
SEM	Scanning Electron Microscopy
POPs	Persistent Organic Pollutants
PCBs	Polychlorinated biphenyl
STP	Standard Temperature and Pressure
TiO_2	Titanium dioxide
TNPs	Titania Nanoparticles
TNTs	Titania Nanotubes
VB	Valence Band
XRD	X-Ray Diffraction
DEHP	Di-(2-ethylhexyl) phthalate

INTRODUCTION

1.1 Background

Plastic is one of the most abundantly used materials worldwide. It is an organic amorphous polymeric solid and its low cost, inertness, thermal and mechanical abilities like durability and versatility make it suitable for many applications. An important type of plastic is polyethylene which has become an indispensible part of modern lifestyle and is being extensively used in domestic, industrial and agricultural sectors resulting increased burden on environment as well as pressure on the capacities available for plastic waste disposal (Shah *et al.,* 2008; Zan *et al.,* 2008).

Polyethylene with an annual global production of around 80 tonnes average is used as packaging material like plastic films, plastic bags, containers including bottles, insulation and geomembranes etc. Use of plastic bags is now considered as an environmental havoc because it takes approximately 1000 years for a polyethylene bag to decompose. Leakage of toxic substances, and blocking of water penetration into the soil are detriment to both the local and extended ecosystem. Ultimately it affects food growth and development (Ellis *et al.,* 2005). Only a very small fraction of the polyethylene bags may be recycled while remaining end up in landfill sites where they would never rot (Panda *et al.,* 2010).

In Pakistan, the plastic industry is growing at annual rate of 15%. According to an estimate, Pakistan's plastic waste generation has reached 1.32 billion tons per annum, out of which 47% remains uncollected and the polythene bags mixed with industrial, animal and human residues became an environmental nuisance. The increasingly higher

component of polythene in solid waste, generated in Pakistan is therefore of considerable attention (Shah *et al.,* 2008).

1.2 Hazards

Polyethylene (PE) waste disposal has been documented as a globally emerging environmental havoc. Over the last few decades, world's water resources like oceans, seas and coastal waters are getting contaminated by non-biodegradable and synthetic materials such as polythene (Sheavly *et al.,* 2007). During rainy seasons, plastic waste causes the blockage of drains and the water overflows. Improperly disposed bags ultimately reaches in water bodies where they kill billions of those marine animals who depends on the oceans for food (Chatterjee *et al.,* 2006). Animals can easily confuse these bags for food as a floating plastic bag look like jellyfish, but are indigestible and can result in injuries or deaths. The bags are so thin and light that they easily ride the wind from landfills to forests, ponds, rivers and elsewhere (Derraik, 2002).

Agriculture sector is one of the biggest user of plastics resulting in thousands of tons of plastic waste annually and most of it is burnt by farmers in uncontrolled manner and releases toxic emissions which poses serious threats to environmental health (Liu *et al.,* 2009). In polyethylene burning process, PE releases many toxic compounds such as aldehydes, methane, ethane and ketones causing serious problems of pollution (Thomas *et al.,* 2013). Plastic bags also serve as mosquito's habitat where they breed and cause malaria (Nerju, 2006).

PE is becoming the serious problem of pollution due to its resistance to enzymatic or microbial degradation and if its degradation aspect will not be addressed, PE cannot continue its essential role to play in usage of our regular commodities (Li *et al.,* 2007).

1.3 Treatment Methods

Various approaches have been established for the elimination of PE plastic waste like incineration, landfills, thermal and catalytic degradation into fuel oil, bio-degradation and photo-catalysis. But most of these methods have some drawbacks associated with them like when plastic is degraded in conventional incinerators, it emits carcinogenic dioxins to the atmosphere (Chakrabarti *et al.,* 2008). Blends and compositions of known biodegradable materials are being produced which can be used as alternatives to non-degradable and inert existing conventional materials. This will ultimately help to solve increasing waste disposal issues that arise from polymer packaging materials (Fontanella *et al.,* 2010).

Solid phase photocatalytic degradation of polymers such as polyethylene (PE) has gained considerable attention in past few years (Liu *et al.,* 2009). Photocatalytic technology using nanostructures as photocatalysts should be a promising way to dispose waste plastics as the process is economical and environmentally friendly (Yuan *et al.,* 2013).

1.4 Proposed Solution

Taking account of what has been discussed above, use of titania nanoparticles and (TNPs) titania nanotubes (TNTs) to degrade polyethylene was selected for the present work. Titanium dioxide is the promising heterogeneous photocatalyst for environmental cleanup due to good photoactivity, high stability, low cost, and non-toxicity (Savinkina *et al.,* 2012).

Detailed studies have been done on modifying titania so that it would be able to absorb light in the visible range (Pan *et al*., 2010). Doping of TNPs with different metals has been commonly used and proved to be a sucessful method in reducing the bandgap of

titania. Dye sensitization of TNPs and TNTs, however, is a comparitively new technique (Fuertes *et al*., 2013) and could be exploited for photocatlytic degradation of polymers.

Dye sensitization is one of efficient methods to enhance the photo response of TiO_2 into visible range of spectrum and has proved one of capable method for utilizing visible light for various environmental benefits, solar cells and so on (Chowdhury et al., 2012). Different dyes have been studied with TiO_2 catalysts for various pollutants degradation under visible light. Visible light driven photocatalytic degradation of phenols, hydrocarbons and chlorophenol with dye sensitized TiO_2 has thus been studied (Chowdhury *et al.,* 2012; Chatterjee *et al.,* 2006; Chatterjee *et al.,* 2001).

At the institute of Environmental Sciences and Engineering (IESE), Asghar (2011) used pure and doped TiO_2 nanoparticles for degradation of polyethylene films. Extending this work, the present study has employed Brilliant Green (BG) dye with titania nanoparticles and nanotubes as catalyst for Low Density Polyethylene (LDPE) films degradation under UV and visible light. The main objective of this investigation was to develop a material that would facilitate the degradation of PE under visible light.

1.5 Objectives

The purpose of this study was to examine the solid phase photo catalytic degradation of low density polyethylene (LDPE) with pure titania and dye sensitized nanaoparticles and nanotubes. More specifically, following were the objectives of this research:

- Synthesis and characterization of pure Titania Nanoparticles and Titania Nanotubes

- Preparation of pure and composite LDPE films

- Characterization of the resulting TNPs, TNTs, pure LDPE and composite LDPE films

- Study of photocatalytic degradation of pure and composite LDPE films under UV and visible light sources

LITRERATURE REVIEW

2.1 Background

Polyethylene is a synthetic resin made from the process of polymerization of ethylene. This white and waxy substance was first produced accidently by Imperial Chemical Industries Ltd. England in 1933 when experiments to study the high temperature effects on the ethylene polymerization were being performed. The process of polymerizing bio-based ethylene is similar to petrochemical ethylene polymerization which has been used at a large scale for many years. The first company which offered bio-based polyethylene at commercial scale was a Brazilian company "Braskem" (Chen and Patel, 2011).

With the passage of time this revolutionary material has changed the world with its applications in various fields of life. It was first used in World War II as an insulating material for military applications like radar insulation and as underwater cable coating. The substance was then a highly guarded secret (Aylward *et al.,* 1999). Thereafter, improved polymer performance and extensive application of technologies expanded the product space and made it applicable for diversified uses nowadays. Polyethylene is a remarkably resistant to degradation and its biological and chemical inertness promoted its wide application (Restrepo-Flórez *et al.,* 2014).

Nowadays, PE is essentially used in food packaging, electronics, industrial storage, transportation industries, consumer goods, power transmission and household goods (Demirors, 2011). It is one of the largest volume polymer produced globally and its production rate has increased from 0.5 million tonnes in 1950 to 260 million tonnes in 2007 with a total of 90 million metric tonnes per annum (O'Brine *et al.,* 2010; Demirors,

2011). Intense use of polymeric materials, however, creates solid waste and disposal issues at the end of their use (Liang *et al.,* 2013). Plastics are also creating visual pollution and are receiving considerable attention nowadays (Fontanella *et al.,* 2010).

2.1.1 Types of plastics

Table 2.1 shows the most common types of plastics used, their applications and their symbols which are often used to identify them on forms of plastic packaging. For the sake of disposal, plastics are placed into seven different groups and given a recycling code based on the material (Chanda and Roy, 2012). Amongst all, PET plastic is mainly used for single-use bottled beverages, because it is easy to recycle and this material is in high demand by remanufacturers. Least recyclable form of plastic is Polystyrene and that is notoriously difficult to recycle (Sadat-Shojai and Bakhshandeh, 2011).

Table 2.1 Different types of plastics with their symbols and uses

Symbol	Polymer Name	Sample Uses
01 PET/PETE	Polyethylene Terepthalate (PET)	Fizzy drinks Mineral water bottles Squashes Cooking oils
02 HDPE	High Density Polyethylene (HDPE)	Detergent bottles, Children's Toys
03 PVC	Polyvinyl Chloride (PVC)	Water pipes, medical equipment
04 LDPE	Low Density Polyethylene (LDPE)	Plastic Bags, packaging e.g. plastic formed around meats and vegetables
05 PP	Polypropylene (PP)	Yogurt containers, screw-on lids
06 PS	Polystyrene (PS)	Plastic cutlery, coffee cups
07 OTHER	Others (All other resins and multimaterials)	Three and five gallon reusable water bottles, some citrus juice and catsup bottles

2.1.2 Types of Polyethylene

Polyethylene has been categorized into three types on the basis of its density governed by branching, crystallinity and most of all its molecular weight. Types of PE are:

- LDPE: Low density polyethylene

- HDPE: High density polyethylene

- LLDPE: Linear low density polyethylene, a mixture of both previous mentioned types

2.2 Low Density Polyethylene (LDPE)

Polyethylene is a flexible synthetic resin as its branched molecular structure prevent it to form stiff, hard and crystalline arrangements. Some of its physical and chemical properties are mentioned in Table 2.2.

Table 2.2 Low density polyethylene properties

LDPE Resistance	LDPE Quick Facts	
Excellent resistance to dilute and concentrated acids	Maximum Temp: 80 ºC Minimum Temp: -50 ºC Autoclave: No Melting point: 120 ºC Tensile strength: 1700 Psi	Hardness: S_D 55 UV Resistance: poor Translucent Excellent flexibility Specific gravity: 0.92
Good resistance to Aldehydes, Ketones and vegetable oils		
Limiting resistance to Aliphatic and Aromatic Hydrocarbons, Mineral Oils and Oxidizing agents		

LDPE has low density due to the presence of small amount of branching in the polymer chain (on about 2% of carbon atoms) which gives a more open structure as shown in Figure 2.1. Low density polyethylene has a high strength to weight ratio, allowing for cheaper transportation costs and lower fuel consumption. Low Density

polyethylene (LDPE) is widely used in manufacturing of wash bottles, dispensing bottles, molded laboratory equipment and most importantly in plastic bags. Polyethylene is resistant to biodegradation due to high molecular weight, hydrophobic nature and the nonexistence of those functional groups which are recognizable by microbes (Roy *et al.*, 2008).
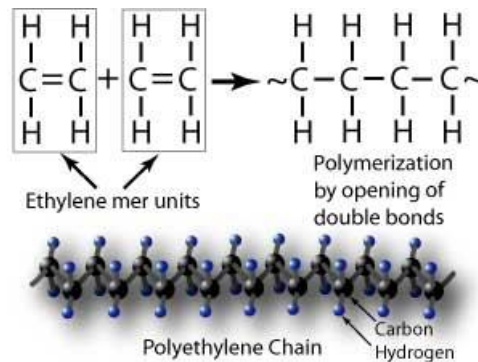
Figure 2.1 Structure of Low Density Polyethylene

2.3 Environmental impacts of Polyethylene

Synthetic polymers like plastics have been entering all marine and land environment in large amounts over the last 50 years. The plastic industry had totally changed general attitude 3 decades back that "*plastic litter is a very minute fraction of the overall solid waste produced globally and have no devastating consequences to the environmental health except as an eyesore*". But the deposition rate has been boosted, past the rate of production in previous few decades and now plastics are considered as most persistent pollutants in oceans, water bodies and beaches worldwide (Thompson *et al.*, 2009). The approximate annual production of plastic bags is about 500 billion worldwide. After USA, Japan, Germany and South Korea, China is the fifth major consumer of plastic consumption which was estimated to be 16 million tonnes in 2000 (Ren, 2003). World's Polyethylene demand is shown in Figure 2.2. Asia is among top users of polyethylene.
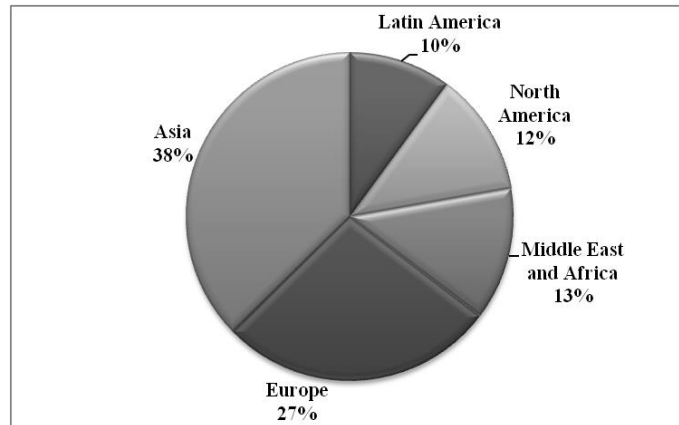
Fig 2.2. Global polyethylene demand in 2013

The ingestion of plastic debris also causes threat to marine life in a new way as chemicals including Polychlorinated biphenyls (PCB's), phthalates and pesticides have been found on plastic samples (Restrepo-Flórez *et al.,* 2014). 267 species of marine organisms worldwide (including sea turtles, cetaceans, filter feeders, sharks, marine birds) are known to have been affected by plastic debris, a number that will increase as smaller organisms are assessed (Thompson *et al.,* 2009). At any garbage dumping site, it can be observed that although other garbage matter gets decomposed and merges into the soil but the PE bags remain intact, with their different colors (Reazuddin *et al.,* 2003).

Polyethylene has been widely used for the protection and cultivation of vegetables and crops and after their use thousands of tons of plastic wastes are disposed of. But major part of this agricultural plastic waste is left on fields or burnt in uncontrolled manner by farmers which contributes to air pollution by emitting harmful substances that leads to negative consequences for the environment (Liu *et al.,* 2009). In landfills, buried plastic waste impedes the soil drainage capacity with deteriorating soil quality resulting in decline in the agricultural yield for our future generations (Liang *et al.,* 2011). A 2002 UN study estimated $7 trillion a year of economic risk from plastic pollution.

Rios *et al.,* (2007) investigated the amount of persistent organic pollutants (POPs) on samples of plastic debris from the Northern Pacific gyre and found that over 50% contained PCBs, 40% contained pesticides and nearly 80% contained PAHs. Teuten *et al.,* (2009) suggested that polyethylene might accumulate more organic contaminants than other plastics. Plastic debris floating on water bodies are continuously threatening navigation, fishery, irrigation, working of hydropower plants and other public tasks. Also, rapid increase in plastics production will put further burden on the already limited nonrenewable resources because over 99% of plastics are of fossil fuel origin (Ren, 2003).

2.3.1 Health impacts

There are several health impacts arising from chemicals either within plastics or transported by plastics waste which can occur due to ingestion, entanglement and improper waste management. Of principal concern are endocrine-disrupting properties, as triggered for example by bisphenol A and di-(2-ethylhexyl) phthalate (DEHP) (Halden, 2010). Plastics are not inert but possess several chemicals which are of toxi potential such as organic pesticides. Plastic debris also has the property to transport contaminants (Mudgal *et al.,* 2011).

The use of PE is also linked to ailments like cancer, skin diseases and other health problems. The consumers are more exposed to these types of health hazards when PE is used to pack bread, biscuits, potato chips or other food items. The hazard is particularly severe in the developing countries where the food is not wrapped in food-graded plastic with colorants, some of which may be carcinogenic (Reazuddin *et al.,* 2003).

2.4 Plastics Degradation

Plastic degradation is defined as detrimental changes in polymer appearance, mechanical, chemical and physical properties resulting due to chemical transformations and bonds scission (Kyrikou and Briassoulis, 2007). Degradation of polymers often starts by fragmentation followed by changes in optical and mechanical characteristics as discoloration, cracking, crazing etc. Polymers are first converted into monomers before they are mineralized. Synthetic plastics degradation in nature is a very slow process taking thousands of years and involves the synergistic action of environmental factors and microorganisms (Ibiene *et al.,* 2014). Degradation of polyethylene is categorized on the basis of the causative process like: (Singh and Sharma, 2008).

- Thermal degradation

- Catalytic degradation

- Ozone induced degradation

- Mechanochemical degradation

- Photo-oxidative degradation

- Biodegradation

Thermal or catalytic degradation needs high temperature which makes it much costly (Li *et al.,* 2007) and degradation of waste plastics in conventional incinerators leads to emissions of global warming gases, carcinogenic dioxins to the atmosphere and divert money and attention from recycling (Chakrabarti *et al.,* 2008). High cost and land shortages for landfills are forcing motivators of alternative options for plastic solid waste disposal (Al-salem *et al.,* 2009).

In biodegradable plastics, microorganisms such as fungi and bacteria are involved in the plastics degradation that decomposes into CO_2, CH_4, H_2O, etc. But Oxi-bio degradation depends heavily on the surrounding conditions (Stevens, 2002; Orhan

and Büyükgüngör, 2000). Scientists researches in the field of degradable plastics is growing, however, they are advised to remain careful because the impacs of degradation products on environment is not clearly revealed yet (Vieyra *et al.,* 2013). Up till now, biodegradable plastics cannot resolve the issue because such plastics have long term degradation limitation, requires aerobic conditions to degrade and cause an environmental problem due to the stabilizers. Furthermore, these are economically not very viable and these bags are not so commonly used by retailers as these have less strength for the same gauge of material (Bonhomme *et al.,* 2003).

Out of all these methods, polymers degradation by photocatalysis such as PE has received considerable attention (Liu *et al.,* 2009). Photocatalysis using nanostructures as photocatalysts could be a promising and environmental friendly way to tackle PE problem (Yuan *et al.,* 2013). Photo catalytic degradation methods for the disposal of plastics is taken in the favor of environment as it do not emits dioxins and the technique is a low temperature process with definite economic advantages (Zan *et al.,* 2006).

2.5 Photocatalytic Degradation Mechanism

Photo-oxidative degradation is the decomposition process in the presence of light which acts as a primary source of damage to polymeric substances (Kumar *et al.,* 2009). Thus, photocatalysis has been described as: *"A change in the rate of a chemical reaction, or its initiation, under the action of UV, visible or infrared radiation in the presence of a substance, the photo catalyst, that absorbs light and is involved in the chemical conversion of the reaction partners without being altered or consumed in the end"* (Braslavsky, *2007).*

Photo-catalytic reactions generally depend upon several factors which affect the kinetics and performance of the photo-catalysis. Some of these factors are: (Herrmann, 2005).

- Catalyst loading

- Physical and chemical properties of Photo-catalyst

- Oxygen pressure

- pH

- Temperature

- Type of light (UV or visible)

- Concentration and type of the organic material

In photocatalytic reaction, initially when radiation of energy equals or exceeds to the band gap of the photocatalyst, a photoexcited electron moves from the filled valence band (VB) of a semiconductor photocatalyst to the empty conduction band (CB) edge leaving a hole in the valence shell (Shan *et al.,* 2010). The valence band hole is strongly oxidizing. Thus, an electron hole pair is generated (e^- -h^+) which migrate to the surface of the semiconductor where they can react with absorbed species leading to following chain reactions (Fujishima *et al.,* 2008).

- Photoexcitation

$$TiO_2/SC + h\nu \quad \rightarrow \quad e^- + h^+ \tag{1}$$

- Oxygen ionosorption

$$(O_2) + e^- \quad \rightarrow \quad O_2^{\bullet-} \tag{2}$$

- Ionization of water : $H_2O \quad \rightarrow \quad OH^- + H^+$ \hfill (3)

- Protonation of superoxides : $O_2^{\bullet-} + H^+ \rightarrow HOO^\bullet$ \hfill (4)

The hydroperoxyl radical formed in last step also has scavenging property as $O_2^\bullet$ therefore increasing the lifetime of photohole: (Hayat *et al.,* 2011).

- $HOO^{\bullet} + e^{-} \rightarrow HO_2^{-}$ (5)

- $HOO^{-} + H^{+} \rightarrow H_2O_2$ (6)
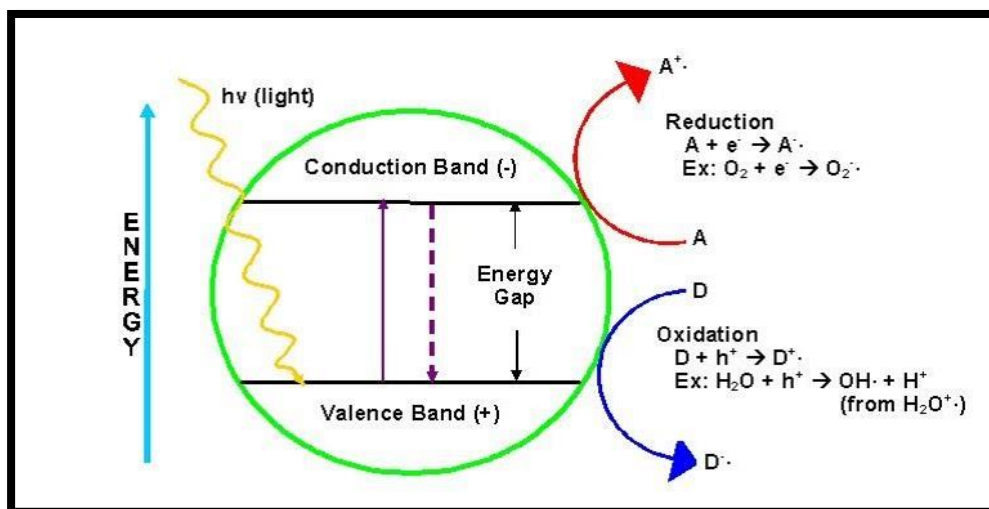
Fig 2.3 Photo-catalysis Process using Titania

The oxidation and reduction, both reactions can take place at the surface of the photoexcited semiconductor photocatalyst as shown in Figure 2.3. Electron and hole recombination occurs unless oxygen becomes available to search the electrons to form superoxides ($O_2^{\bullet-}$), its protonated form the hydroperoxyl radical ($HO_2^{\bullet}$) and afterward H_2O_2 (Nath *et al.,* 2012).

2.6 Photocatalyst

Photocatalyst is usually a solid and semiconductor in nature, not consumed during a reaction. The semiconductor commonly used is chemically stable, cost effective and capable of reuse without losing its catalytic ability. An ideal photocatalyst should exhibit a narrow band gap thus being photoactive under visible light. Most importantly, it should be non-toxic to both man and environment (Bhatkhande *et al*., 2002). Upto now heterogeneous semiconductor materials like ZnO, Fe_2O_3, CdS, ZnS, TiO_2, SnO_2, WO_3, $LiNbO_3$ are used as photocatalyst, but one of most widely used photocatalyst is TiO_2 (Nath *et al.,* 2012).

2.6.1 Titania as Photocatalyst

As mentioned above, a photocatalyst is that substance which induces chemical reaction after being irradiated by light but such a substance itself will not be consumed in that reaction. TiO_2 is a white odorless and noncombustible powder with melting point of 1843 °C, boiling point of 2972 °C, MW of 79.9 g/mol and relative density of 4.26 g/cm^3 (Shi *et al.,* 2013). Among various types of photocatalysts, TiO_2 is the most commonly used semiconductor for organic pollutants degradation (Shan *et al.,* 2010). In the twentieth century, titanium dioxide has also been widely used in many commercial applications like as pigments, ointments, toothpastes, sunscreens and paints etc. (Chen and Mao, 2007).

Titania photocatalysis was first described by pioneering research of Fujishima and Honda and referred as "The Honda–Fujishima effect" (Gaya and Abdullah, 2008). The oxidizing of titania depends on the energy level of the valence band. The VB of titania is reported to be 3.2 eV (which corresponds to the wavelengths in the range of ultraviolet light) so it acts as a strong oxidizing agent, which can simulate various photochemical reactions (Zhao *et al.,* 2005). Hence, TiO_2 is the promising photocatalyst for environmental cleanup due to (Savinkina *et al.,* 2012):

- Most efficient photoactivity

- Good stability

- Inertness

- Corrosion resistant

- Lowest cost, and

- Absence of toxicity

Titania photocatalysis goes through oxidative or reductive reactions under UV light to produce $O_2^{\bullet-}$, $HO_2^{\bullet}$, $HO^{\bullet}$ from H_2O or O_2 which further lead to polymer

degradation reaction by breaking the polymer chain and following chain cleavage (Cho and Choi, 2001; Kim *et al.,* 2006).

2.6.2 Polymorphs of TiO$_2$

TiO$_2$ belongs to transition metal oxides family. There are three commonly known crystalline forms of titania found in nature: anatase (tetragonal), brookite (orthorhombic) and rutile (tetragonal). TiO$_2$ is a large band semiconductor, with band gaps of 3.2, 3.02, and 2.96 eV for the anatase, rutile and brookite phases, respectively (Gupta & Tripathi, 2011). Among these, anatase tends to possesses highest photoactivity and remain stable at tempratures less than 700 $^{\circ}$C. Unit cells for these three TiO$_2$ polymorphs are shown in Figure 2.4.
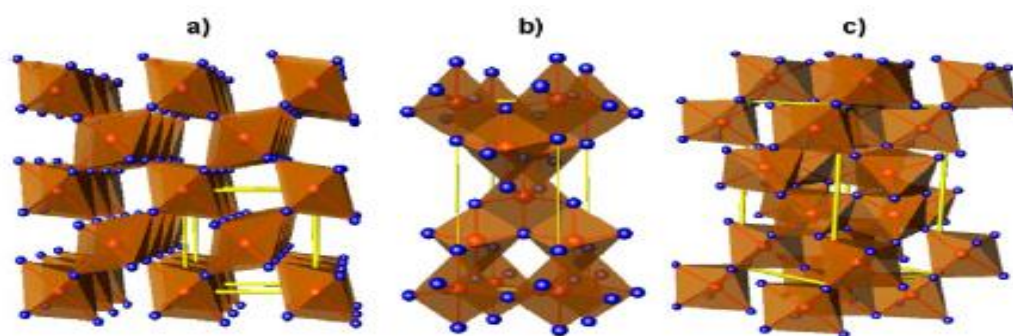
Figure 2.4 Crystal structures of TiO$_2$ polymorphs. (a) Rutile. (b) Anatase. (c) Brookite (Fuertes *et al.,* 2013).

Two polymorphs of titania, anatase and rutile are used for exhibitng photocatalytic activities rather than rutile phase because anatase phase has 80 cm^{2}V^{-1}s^{-1} charge carrier mobility which is 89 times higher than the rutile phase (Woan *et al.,* 2009). The manufacturing processes for amorphous and other titania crystalline forms (anatase/rutile/brookite) are (Fröschl *et al.,* 2012):

- Electrodeposition
- Solvo or hydrothermal methods

- Microwave treatments

- The hydrolysis of $TiCl_4$

- Flame pyrolysis of $TiCl_4$

2.6.3 Drawbacks of TiO$_2$

Pure TiO_2 has a large band gap due to which it cannot be activated until irradiated with photons of UV domain ($\lambda \leq 385$ nm for anatase). It limits the solar light's practical applications. The recombination of the photogenerated electron–hole pairs takes place quickly on a time scale of 10^{-9} to 10^{-12} s (Gratzel, 2005). There is need to develop an efficient and visible light responsive photocatalyst in order to improve the photocatalysis process.

2.7 Novel photocatalyst preparations

Due to the constraints involved in ensuring effective photoactivation, there has been growing pursuit to go beyond the threshold wavelength of 385 nm which corresponds to the band gap of titania. The principal pivot of these activities include: (Gaya and Abdullah, 2008).

- Incorporation of energy levels into the band gap of the titania

- Replacement of the Ti^{4+} with same size cation

- Changing the life time of charge carriers

- Shifting the conduction band and/or valence band so as to enable photoexcitation at lower energies

2.8 Titania Nanoparticles

Titania nanoparticles are those particles which have at least one of their three dimensions in the nano range of 1 - 100 nm. TNPs have enhanced photocatalytic activity due to their good enough surface area and being predominantly anatase phase (Shi *et al.,* 2012). TNPs are much effective as photocatalyst rather than bulk powder form (Gupta & Tripathi, 2011). These have been widely used in photocatalysis, sewage and water treatment, antibacterial materials, solar cells, cosmetics, air purification, self-cleaning windows, self-cleaning tiles and anti-fogging car mirrors (Montazer & Seifollahzadeh, 2011; Yuan *et al.,* 2010; Ni *et al.,* 2011). There are numerous methods to synthesize TNPs i.e. microemulsion, physical vapor deposition (PVD), hydrolysis, hydrothermal, sol-gel and liquid impregnation (Bagheri *et al.,* 2013).

Liquid Impregnation (LI) method involves the mixing of TiO_2 in water. Only stirring is required during the process. Liquid impregnation method is a low cost technique, shows very good reproducibility and requires simple apparatus to synthesize TiO_2 (Behnajady *et al.,* 2008; Khan *et al.,* 2013).

2.9 Titania Nanotubes

In most of the photo-catalytic processes, high surface area and finest pore size are needed for active sites interaction and reactive species diffusion. This condition is satisfied by titania based nanorods, nanotubes and nanowires (Asapu *et al.,* 2011). The problem regarding planar surface like nanoparticles was the optical loss i.e. photons of light required to excite the photocatalyst. Planar surface is unable to utilize maximum photons for its excitation. Titania nanotubes (TNTs) are now gaining importance in the process of photo-catalysis due to their tremendous chemical and physical properties like

- High surface area

- Better photo-catalytic activity

- Widespread availability

The use of titania nanotubes is known to improve efficiency due to directional electron transport, which is a function of many factors including: (Butail *et al.,* 2012)

- Nanotube length

- Wall thickness

- Pore diameter and

- Fabrication conditions

As nanotubes have large surface area, these provide paths for enhanced electron transfer, ultimately helping to increase the photocatalysis efficiency. Titania nanotubes are also very resilient during heat treatment so their application as photocatalyst is strikingly good (Wong *et al.,* 2011).

2.9.1 TNTs Synthesis

There are various methods reported to prepare Titania nanotubes using techniques like

- Molecular assembly

- Replica or template synthesis method

- Sol gel

- Anodization

The scenario of fabrication approaches for TiO_2 based nanotubes is demonstrated in Figure 2.5. Some of these techniques however, are not able to yield crystallized, well separated and low dimensional nanotubes (Poudel *et al.,* 2005).

| Template Method, 1996 |
| Sol-gel process, 1998 |
| Hydrothermal Method, 1999 |
| Anodic Oxidation, 2001 |
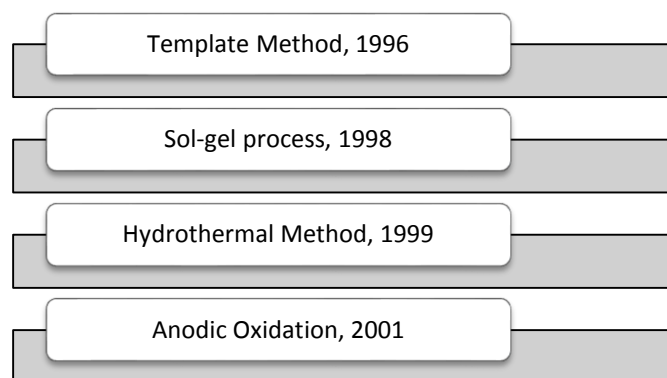
Fig 2.5 Various fabrication methods in TiO₂ based nanotubes.

TNTs can be easily produced by very easy and efficient hydrothermal method under moderate conditions of pressure and temperature (Wong *et al.,* 2011). In this hydrothermal method, nanotubes can be produced through simple wet chemical synthesis routes and at low temperatures (Asapu *et al.,* 2011).

2.9.2 Formation mechanism of TNTs: Hydrothermal method

Various chemical methods have been reported for titania nanotubes synthesis, out of which a method introduced by Kasuga and coworkers received much attention because that method was successful for producing thin walled nanotubes (Wang *et al.,* 2004). This method is convenient, environmentally innocuous and inexpensive for producing high quality TNTs. The hydrothermal method is usually recommended for commercial production of TNTs (Vijayan *et al.,* 2010).

In this method, hydrothermal reaction of NaOH as a strong base break the Ti-O-Ti bonds. The hydroxyl bridges are formed by sharing edges of free octahedral shapes Ti ions. This results in a zig-zag structure. In autoclave, the titanate sheets desquamate into nanosheets having 1 or 2 layers which further roll into nanotubes at slow rate with one or two layers, and then the nanosheets rolled into nanotubes at slow rate in presence of high concentration of NaOH (Yuan & Su, 2004). Also rolling of crystalline sheet helps to saturate surface dangling bonds, which lower the total energy and TiO₂ nanotubes forms

(Chen and Mao, 2007). The final tubular structure is obtained after 20 h of reaction time. Nanotubes washing with water and dilute acidic solution removes sodium ions attached in nanotubes but sodium salt can be found if sample is not well washed (Brunatova *et al.,* 2014).

The hydrothermal reaction of anatase titania with concentrated solution of NaOH at 100 – 160 $^\circ$C temperature, results in nanotubes production, on the other hand amorphous TiO_2 treated under same experimental conditions results in nanofibers production (Yuan & Su, 2004). Hydrothermal synthesis is an environmental friendly technique as this reaction takes place in aqueous solution at low temperature within a closed system such as autoclave. Also this method is widely accepted for TNT systhesis because of other aspects like low temperature need, high reactivity, pollution free setup and easy control of aqueous solution (Wong *et al.,* 2011). Hydrothermal soft chemical method involving titania nanoparticles in anatase phase with NaOH treatment followed by acid washing is a relatively effective route for nanotubes production (Huang and Chien, 2013).

2.9.3 Calcination of TNTs

Xu and cowokers in 2011 analyzed their synthesized nanostructures by XRD, Raman spectroscopy, SEM and high resolution TEM. They found that after the calcination process, the prepared nanotubes turned into anatase phase different from the original structure. Their results further revealed that such nanotubes show better photo-catalytic activity than the amorphous ones due to improved crystallinity (Xu *et al.,* 2011). TNTs are stable at temperature less than 400°C but exceeding calcinations temperature beyond 540°C change these into nanorods having a circular cross section.

2.10 Dye Sensitization

Titania as photocatalyst is only active in UV range ($\lambda < 385$ nm) so to activate it in visible range which is about 43% of solar spectrum, there is need to alter the bulk or surface properties of TiO_2 (Li *et al.,* 2012). Considerable efforts and techniques have been made to utilize visible part of solar light and to modify the surface or bulk properties of TiO_2 such as doping with various metal ions or nonmetals, metal and non-metal codoping and mixing of two photocatalysts (Xue *et al.,* 2011).

Most of these methods are costly and time-consuming. Whereas dye sensitization is effective method to enhance the photo response of TiO_2 into the visible range and proved as promising method to harness visible light for environmental applications and solar cells etc. (Chowdhury *et al.,* 2012). Any shift of optical response in the visible wavelength range due to doping TiO_2 with metals or non-metals, sensitization of TiO_2 with organic dyes relatively narrow bandgaps (less than that of TiO_2), gives a positive effect for photocatalysis (Struzhko *et al.,* 2011).

In TiO_2 photosensitization, dye molecules absorbed on TiO_2 surface are excited by visible light and inject electrons into the conduction band (CB) of TiO_2 as shown in Figure 2.6. In the next step, dioxygen adsorbed on the surface of TiO_2 reacts with injected electrons and produces a series of reactive oxygen species such as $O_2^{\bullet-}$, $HO_2^{\bullet}$, $HO^{\bullet}$ which further degrade target pollutants (Li *et al.,* 2012).
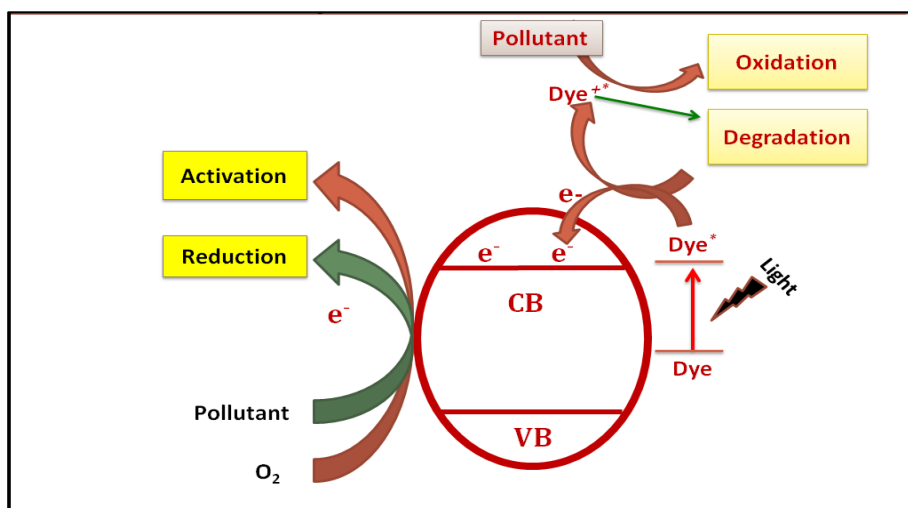
Fig 2.6 Involved radical reactions during the dye sensitized photocatalytic degradation (Park *et al.*, 2010).

A number of dyes (eosin Y, rhodamine B, thionine, methylene blue, brilliant green safranine O and nile blue A) have been studied with TiO_2 photocatalysts for pollutants photo-degradation under visible light (Chowdhury *et al.,* 2012; Chatterjee *et al,* 2001; Chatterjee *et al.,* 2006). Some ruthenium complexes have also been used to sensitize TiO_2 for the degradation of halogen-containing organic compounds and nitrogen oxides (Li *et al.,* 2012).

2.11 Dye-Sensitized TiO_2 Nanotubes and Nanoparticles

The usage of large band gap nanostructures semiconductor for the purpose of solar energy conversion is an emerging area of research (Zhang *et al.,* 2008). Dye sensitization of titania structures to harness visible energy have been observed in various studies. Chowdhury and coworkers used Eosin Y dye as a sensitizer for the TiO_2 catalyst with platinum as a cocatalyst for the photo catalytic degradation of phenol under visible solar light and 93% degradation of phenol was achieved using Eosin Y−TiO_2/Pt photocatalyst (Chowdhury *et al.,* 2012). In a study by Chaterjee and Mahata, a pesticide

has been degraded in air-equilibrated aqueous mixture under visible light by modifying the surface of TiO_2 with thionine and eosin Y dyes (Chatterjee & Mahata, 2004).

Fa and coworkers modified the titania photocatalyst by iron (II) phthalocyanine for improving its photocatalytic efficiency for solid-phase photocatalytic degradation of polystyrene under visible light (Fa *et al.,* 2008). Wang and Lin prepared TiO_2 nanotube arrays and sensitized these with ruthenium dye N-719 to obtain dye sensitized TiO_2 nanotube solar cells and achieved power conversion efficiency up to 7% (Wang and Lin, 2009). Macak and coworkers used ruthenium based dye (N3) to sensitize self-organized TiO_2 nanotubes and reported that TiO_2 nanotubes can be dye-sensitized in the visible range with a considerable light conversion efficiency (Macak *et al.,* 2005).

2.12 Brilliant Green Dye

Brilliant Green (BG, Bis (4-diethylaminophenyl) phenylmethylium chloride) dye is used to color silk and wool and has been used as a topical antiseptic in Eastern Europe and Russia. BG dye has chemical formula = $C_{27}H_{34}N_2O_4S$, FW = 482.62 g/mol; Dye content = 85%, nature = basic green 4. Absorbance of standard solution of dye was measured via UV-Vis spectrophotometer which was 623nm as reported elsewhere (Mane *et al.,* 2007). The structure of BG is presented in Figure 2.7.
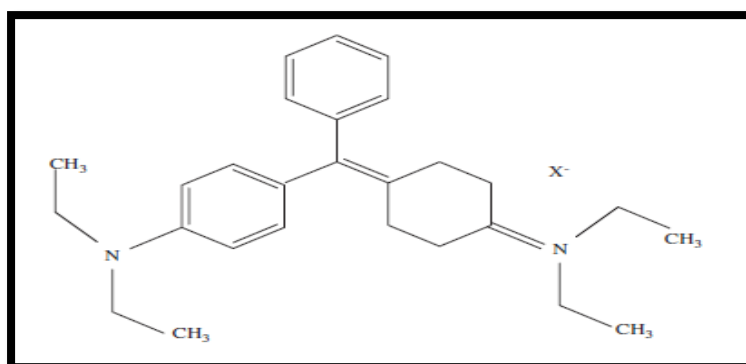
Fig 2.7 Molecular Structure of Brilliant Green (Mane *et al.,* 2007)

In previous studies, brilliant green dye have been used to sensitize titania monoliths and the optical properties of amorphous TiO_2 monoliths doped with brilliant green dye have been reported (Tomas *et al.,* 2008).

2.13 Photocatalytic Degradation Mechanism of PE

One most important factor which decides most damaging UV wavelength for different types of plastics is the presence of different bonds therefore maximum degradation occurs at different wavelengths for different plastics i.e. 370 nm for polypropylene (PP) and around 300 nm for polyethylene (PE) (Singh & Sharma, 2008). Photocatalytic degradation of PE is only stimulated by UV light due to presence of C-C and C-H bonds in Polyethylene as shown in Figure 2.8. The wavelength of UV light is in the range of 200 to 390 nm which forms macromolecule radicals as holes and electrons centers after reacting with PE. Water or oxygen react with these electron or holes to create active oxygen species leading to the chain cleavage, branching cross linking and oxidation reactions. These active oxygen species such as ·OH and O_2^- are initiators of photocatalytic degradation of PE in solid phase by attacking the polymeric chain (Fa *et al.,* 2010; Zan *et al.,* 2008).
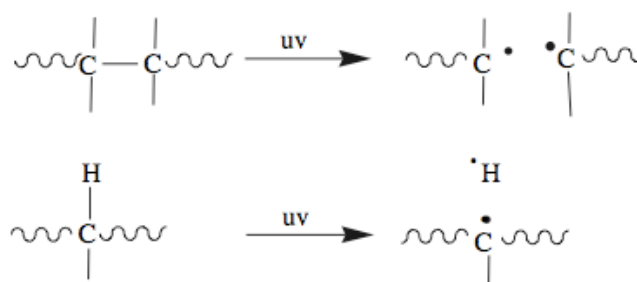
Fig 2.8. Illustration of UV radiation disassociating bonds in photo-oxidative degradation

Basically, photolysis of PE gains momentum by impurities such as carbonyl groups and alcohol (Zan *et al.,* 2006). It is proposed that in PE-(BG-TNPs or TNTs), holes generated in the ground state of BG dye plays an essential role also with $^{\bullet}OH$ and O_2^-. Better holes production occurs at ground state of brilliant green dye on titania surfaces which makes it favorable to take part in oxidation of PE matrix.

$$h^+ + (CH_2CH_2)- \longrightarrow -(CH_2CH_2)-^+$$

$$-(CH_2CH_2)-^+ + O^{2-} \longrightarrow -(C^{\bullet}HCH_2)- + HO_2^{\bullet}$$

$$HO_2^{\bullet} + HO_2^{\bullet} \longrightarrow H_2O_2 + O_2$$

$$H_2O_2 \xrightarrow{h\nu} 2^{\bullet}OH$$
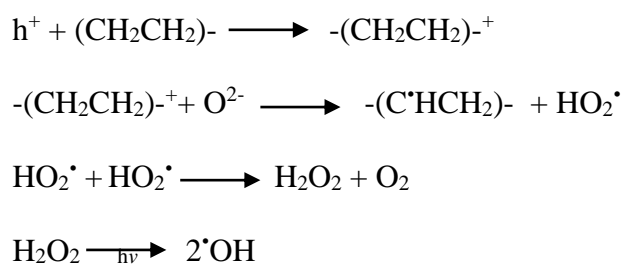
The embedded BG-TiO_2 can thus generate more $^{\bullet}OH$ to photodegrade the LDPE matrix. The damaging effects caused due to photo-oxidative degradation can be noted visually like yellowing while the polymers mechanical properties and molecular weight gets changed (Singh & Sharma, 2008).

2.13.1 Photo-absorbing chromophores

To start the photodegradation process, the UV radiation has to be absorbed by PE film. The presence of photo absorbing chromophores make possible the absorbtion of UV radiation in PE. Chromophores is that group which is responsible for a given absorbtion band and may come from the polymerisation catalysers, polymerisation process and additives such as lubricants, stabilisers and plasticisers, etc (Briassoulis *et al.,* 2004). One group of chromophores (containing carbonyls) can also be used to monitor degradation by monitoring carbonyl groups in LDPE films.

Once free radicals are formed in the initiation step, the photo-oxidation process propagates, giving rise to various oxidation products and finally leading to degradation of the PE film. After free radicals formation in initial step, photo-oxidation process

promotes, which produces various oxidized species and finally leads to the LDPE films degradation.

2.14 Previous work on Photo-degradation of LDPE

Some work has already been done on degradation of low density polyethylene which also supports the use of titania as photocatalyst. TNPs have been used in many other studies to photo degrade polymers (Zhao *et al.,* 2006; Zhiyong *et al.,* 2007; Zhao *et al.,* 2008; Asghar *et al.,* 2011; Thomas *et al.,* 2013; Liang *et al.,* 2013). Zan and coworkers made low-density polyethylene (LDPE)-TiO$_2$ nanocomposite film by melt blending method and found weight loss of nanocomposite upto 68% under visible light irradiation in 300 hrs (Zan *et al.,* 2006). Li *et al.,* 2007 carried out solid-phase photocatalytic degradation of polyethylene plastic under UV and solar light irradiation and reported weight loss of PE-TiO$_2$ film up to 42% under solar irradiation in 300 h.

In another study, Zhiyong *et al.,* 2007 investigated photocatalytic applications of LDPE-TiO$_2$ composite film irradiated for 10 h and showed higher compactness after the photocatalysis. Another study conducted by Zhao and coworkers reported improvement in photocatalytic degradation of polyethylene plastic by TiO$_2$ modified with copper phthalocyanine (CuPc) and got better photocatalytic degradation than PE–TiO$_2$ composite films (Zhao *et al.,* 2008).

A study has been conducted on solid-phase photo catalytic degradation of polythene goethite composite film under UV light and found out that degradation of composite film was much faster and more complete by goethite particles in PE plastic (Liu *et al.,* 2009). A study has also been conducted on Polyethylene degradation at IESE by Asghar *et al.,* (2011). According to his work polyethylene films containing nanoparticles degraded by photocatalysis with the weight loss reduction reaching upto

14% under UV light with doped TiO_2 nanoparticles and 14% weight loss under visible light with silver doped TiO_2 nanoparticles in 300 h.

In one recent study by Thomas *et al.,* (2013), TiO_2 nanoparticles assisted solid phase photocatalytic degradation of polythene film was carried out and found that titania nanoparticles prepared with sol gel method gives enhanced photocatalytic degradation. Similarly, Liang and coworkers prepared low density polyethylene by embedding with polyacrylamide grafted titania nanocomposite and high photocatalytic degradation of films was observed under UV irradiation (Liang *et al.,* 2013).

Most of the studies in this regard are restricted to use of nanoparticles only and no work has been done on nanotubes to the best of our knowledge. These studies however provide a baseline for using titania photocatalyst with high surface area.

MATERIALS AND METHODS

3.1 Materials

Cyclohexane (Merck, Germany), Hydrochloric Acid, Sodium Hydroxide, GPR TiO_2 (Sigma Aldrich Laborchemikalien) and dyes like Brilliant Green were used in this study. Low-density polyethylene (LDPE) pellets were purchased from the local market. Analytical grade chemicals and Pyrex glassware was used. Double distilled water was used in all the experiments.

For photo-catalytic experiments, visible lamps of 85W with a wavelength range of 400-700 nm were used as a light source. Two 18W Ultraviolet lamps (primary wavelength of 315 nm) were also used to carry out photo-catalytic activity below 400 nm. pH meter (CyberScan 500 Eutech) was used to measure pH of the dye solution. ABM Model 150 digital intensity meter was used for light intensity measurement.

3.2 Nanostructures synthesis

3.2.1 Synthesis of TiO_2 Nanoparticles (TNPs)

For the synthesis of TNPs, 20 g General purpose reagent (GPR) was added in 100 ml distilled water and stirred for 24 h on a magnetic plate. The resulting solution was allowed to settle and then dried in oven at 105 ^{o}C for 12 h. The dried sample was then crushed and calcined in a muffle furnace at 450 ^{o}C for 6 h to get TNPs which changed the crystalline form of titania from amorphous to anatase. The resulted sample was allowed to cool at room temperature to get TNPs (Khan *et al.,* 2013). Resulting TNPs were in the range of 39 to 80 nm with average size of 50 nm.
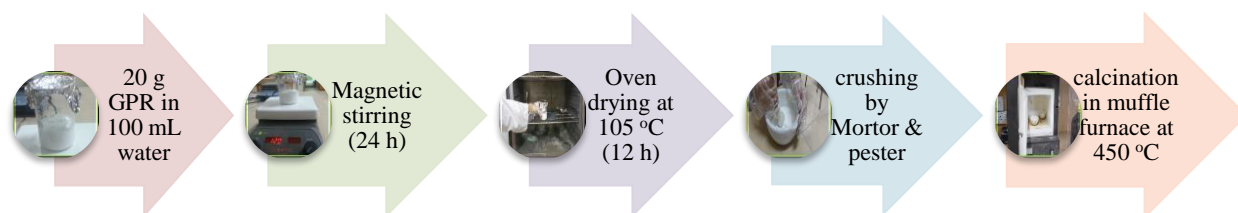
Fig 3.1 Flow sheet diagram of TiO$_2$ nanoparticles preparation

3.2.2 Synthesis of TiO$_2$ nanotubes (TNTs)

In present study, pure TNTs were synthesized by the hydrothermal method. For the preparation of Titania nanotubes, TNPs were used as a precursor. For this purpose, 2.5 g prepared TNPs were added in 100 ml of 10 M NaOH solution and stirred for 2 h followed by 1 h sonication. The resulted material was then transferred into Teflon lined autoclave at 135°C for 24 h with continuous stirring at 350 rpm. After time completion, sample was extracted, cooled at room temperature and washed with 0.1 M HCl and then distilled water several times until the pH of solution becomes neutral (7). After washing, the solution was dried in hot air oven for 24 h at 105 °C. The sample was then ground into fine powder. In last step, the sample was calcinated in a muffle furnace at 500 °C for 1 h in order to obtain TNTs in maximum crystalline form (Asapu *et al.,* 2011; Lee et al., 2009).
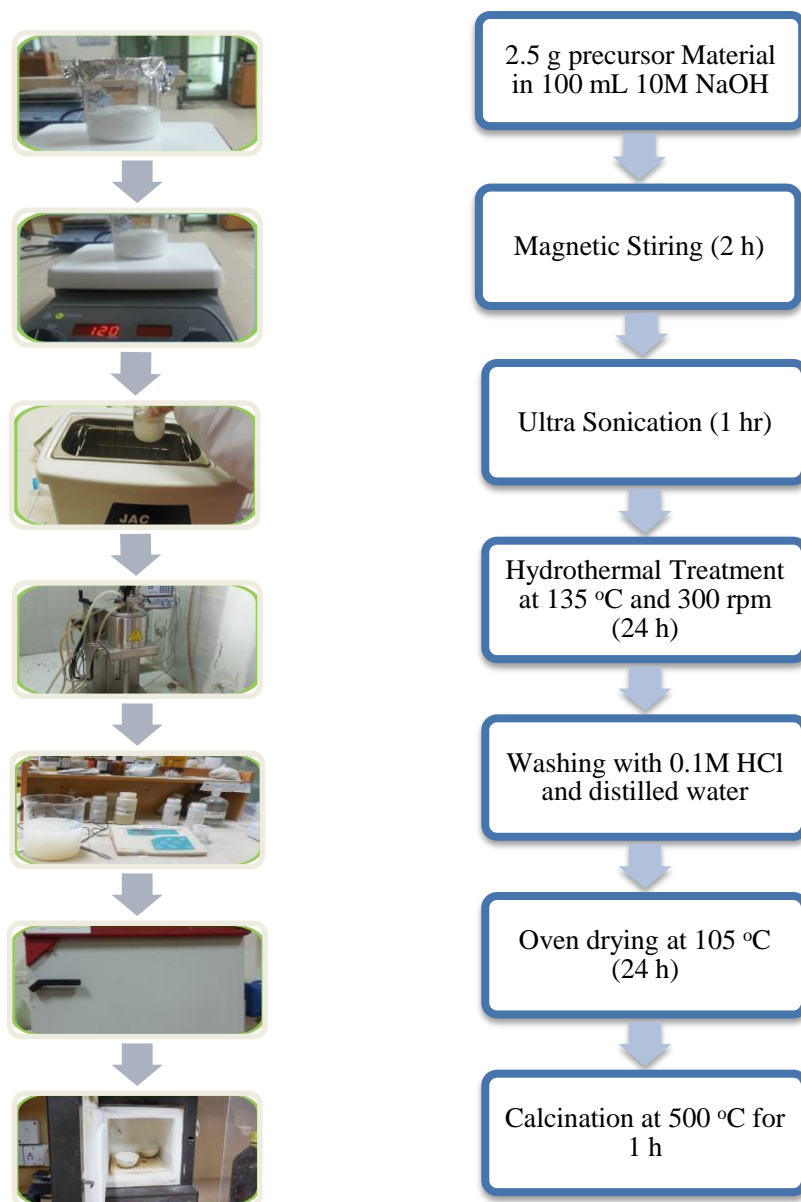
Fig 3.2 Flow sheet diagram of TiO₂ nanotubes preparation

3.3 Preparation of dye sensitized photocatalysts

Required amount of TNPs or TNTs were soaked in 0.1 M HCl for 6 h. For preparation of dye sensitized photocatalyst, saturated solution of brilliant green dye (pH~ 3) was made in 100 ml of ethanol and 500 mg of TNPs or TNTs were added separately. Samples were stirred on magnetic stirrer for 24 hours in dark to homogenize the dye and gain maximum absorption/desorption equilibrium. Samples were filtered via filter paper and the filtered TNPs or TNTs were separated and washed with distilled water. Hence

Brilliant Green dye Sensitized photocatalysts were obtained (Chatterjee & Mahata, 2001; Mack *et al.,* 2005).
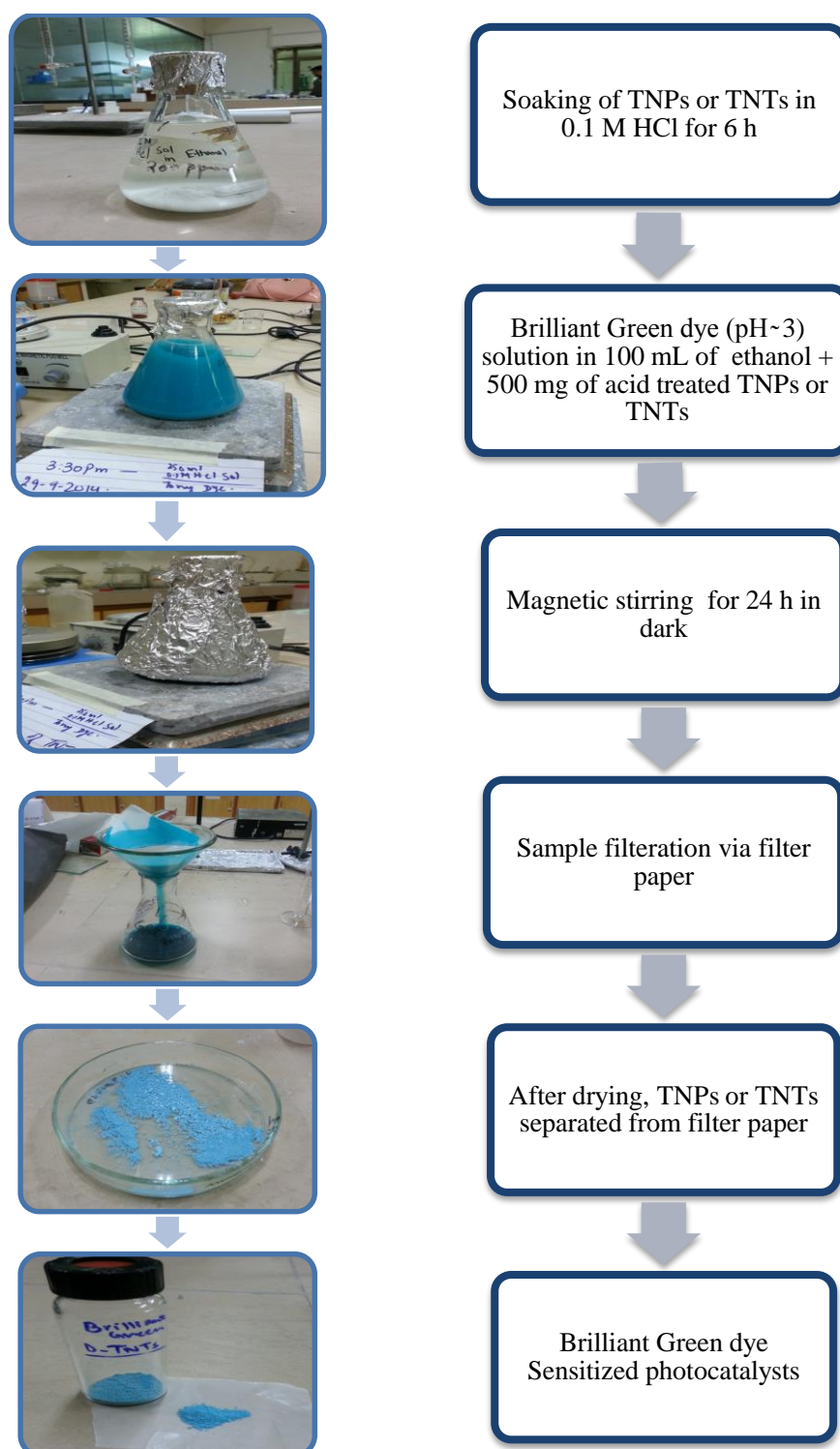
Fig 3.3 Flow sheet diagram of TiO$_2$ dye sensitized photocatalyst preparation

3.4 Preparation of pure and composite LDPE Films

The stock solution of polymer was prepared by dissolving 0.5 g of LDPE in 50 ml cyclohexane at 70 °C under fast stirring for 90 minutes.
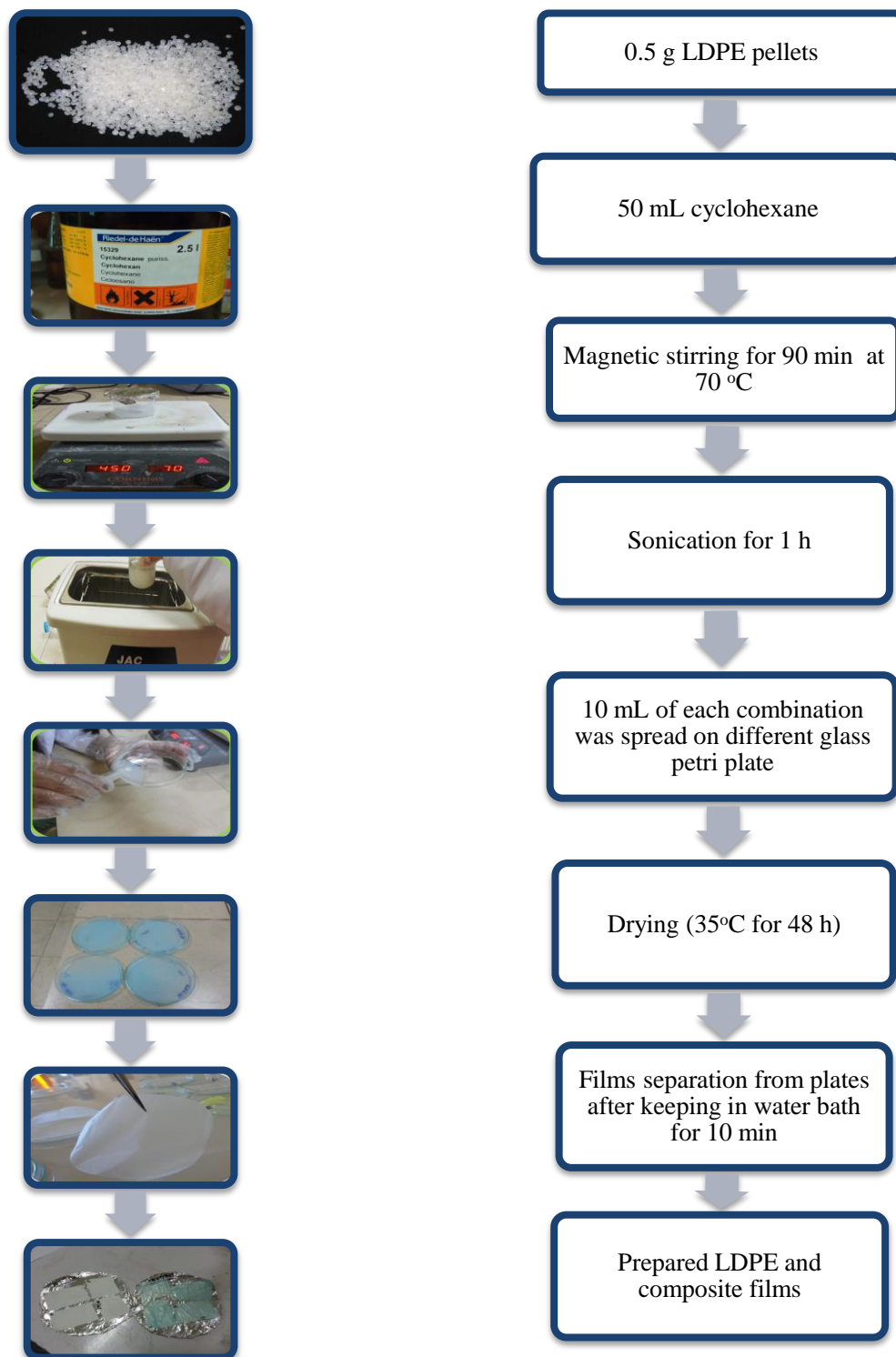
Fig 3.4 Flow chart for preparation of pure and composite LDPE Films

10 mL of the LDPE suspension was spread on glass petri plate to get pure LDPE film. Composite LDPE films were prepared by dissolving the required amount of TNPs, TNTs or dye Sensitized TNPs or TNTs (1, 2, 7, 10 and 15%) in the LDPE suspension and after one hour of ultra-sonication, 10 mL of each combination was spread on different glass petri plate. All films were dried for 20 min at 70 °C, and kept to be dry at room temperature for 48 h. Films were separated by placing in a water bath at 70 °C for 10 min. Details of pure and composite PE films are given in Table 3.1. Three replicates of each type of LDPE composite was taken and average was noted. Weight of the resulting composites was around 0.02 g and the thickness was about 0.024 mm.

Table 3.1 Details of pure and composite LDPE films

S #		% of nanostructures by weight in LDPE films	Weight (gm)	Thickness (mm)
1	**Pure LDPE**	-	0.0150	0.024
2	**TNPs**	1%	0.0201	0.030
3		2%	0.0172	0.025
4		7%	0.0171	0.029
5		10%	0.0194	0.026
6		15%	0.0195	0.021
7	**TNTs**	1%	0.0187	0.020
8		2%	0.0184	0.025
9		7%	0.0221	0.023
10		10%	0.0205	0.025
11	**BG-TNPs**	1%	0.0197	0.027
12		2%	0.0113	0.023
13		7%	0.0204	0.029
14		10%	0.0204	0.028
15		15%	0.0229	0.025
16	**BG-TNTs**	1%	0.0194	0.026
17		2%	0.0197	0.024
18		7%	0.0194	0.022
19		10%	0.0197	0.022

3.5 Experimental Setup

Photocatlaytic degradation of LDPE and composite films was carried out under UV light irradiation for 15 days in ambient air with a distance of 5 cm from the light source. After UV light experiments, visible light experiments were carried for 45 days under same conditions. The average size of films was 3cm x 3cm and 0.024 mm thickness. These films were constantly irradiated for 45 days in a closed wooden box (90 cm $\times$ 50 cm $\times$ 50 cm) containing lamps as shown in Figure 3.5. Actual setups for visible and UV light photodegradation are shown in Figures 3.6 and 3.7 respectively.
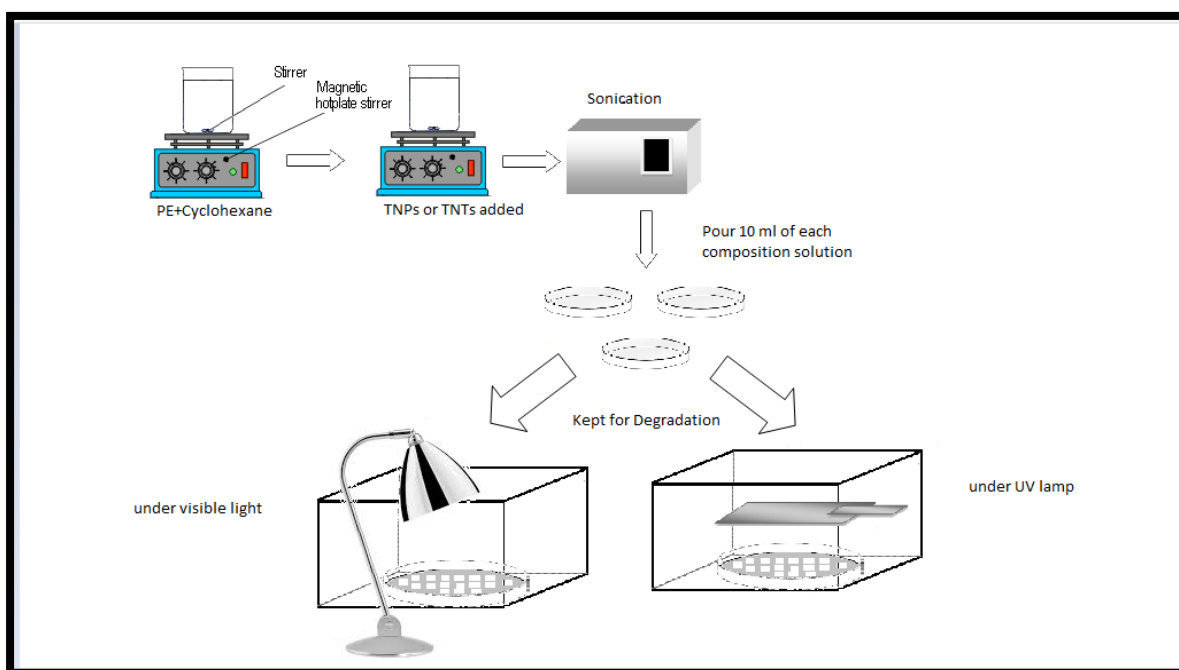
Fig 3.5 Experimental setup for Photo catalytic degradation of LDPE films

Fig 3.6. Setup for photocatalytic degradation of LDPE composite films under visible light
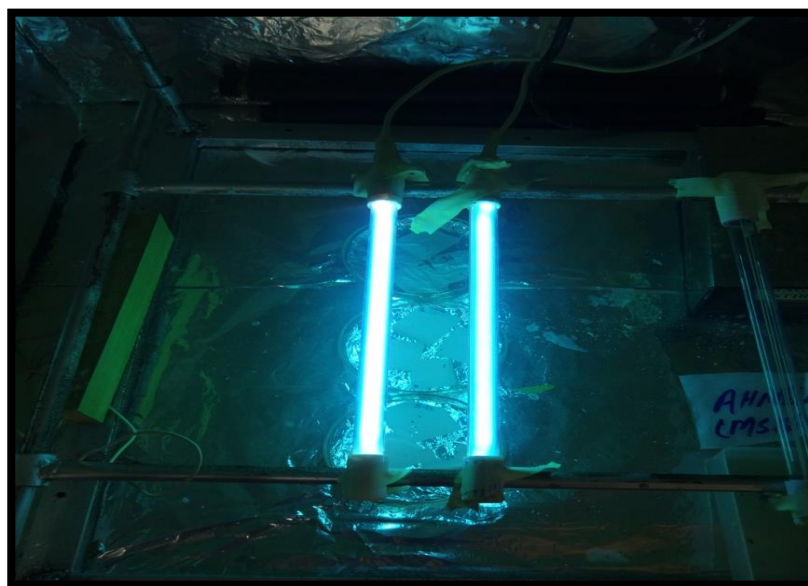
Fig 3.7 Setup for photocatalytic degradation of LDPE composite films under UV light

Light intensity was 2.546 mW/cm^2 for UV lamps and 6.76 mW/cm^2 for visible lamp at 5cm away from sources. Each sample was weighed after every three days during 45 days of irradiation. All the experiments were conducted under visible as well as UV

light and finally a comparison study was done among the different samples of titania to find out the conditions best suitable for the photocatalytic degradation of LDPE.

3.6 Characterization of nanostructures and PE films

Considering the role of shape and size of nanoparticles and nanotubes in their application, characterization techniques for nanostructures becomes crucial which can determine their surface texture, structure and size. Generally the techniques which are common for characterization are scanning electron microscopy (SEM), Fourier transform infrared spectroscopy (FTIR) and powder X-ray diffractometry (XRD) (Choi *et al.,* 2010; Yoosaf *et al.,* 2007). With the use of these techniques, other important parameters can also be determined such as pore size, crystallinity, surface area and fractal dimensions. In addition to this, intercalation and dispersion of nanoparticles and nanotubes in a nanocomposite films can also be detected. SEM is useful for surface morphology studies. Crystallinity of particles and tubes can be obtained by using x-ray diffraction (Abou El-Nour *et al.,* 2010).

3.6.1 Morphology (SEM)

SEM stands for scanning electron microscope. In SEM, electrons are used to form an image instead of light. Since its discovery in 1950's, SEM has been extensively used in various fields of medical and physical applications. The SEM has much higher resolution and user has much control in the degree of magnification so specimens can be examined at much higher levels with strikingly clear images (Essers, 2003). The actual working phenomenon of SEM is given in Figure 3.8.
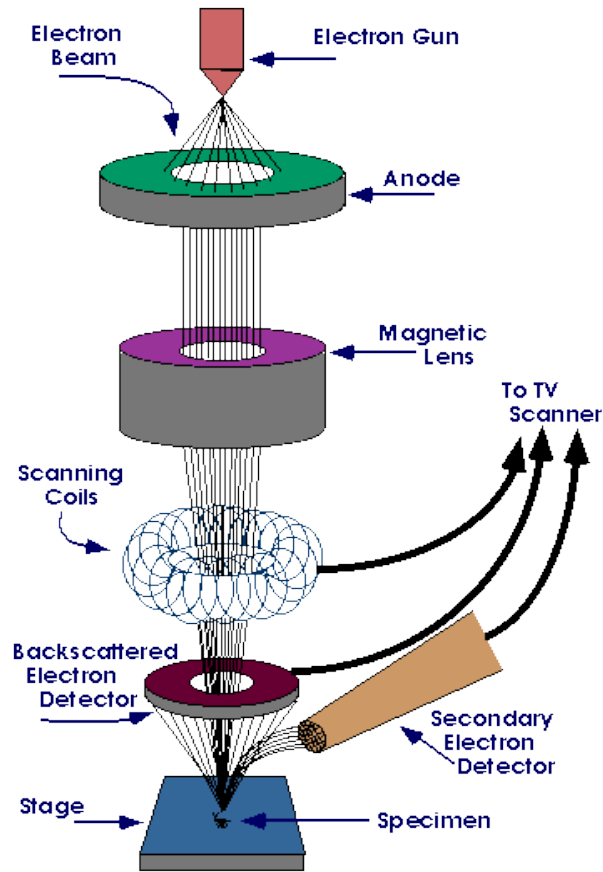
Fig 3.8 Working principle of Scanning Electron Microscope

Electron gun produces electrons beam at the top of microscope which makes a vertical path to follow in the microscope and it is held within a vacuum. Beam passes through electromagnetic fields and lenses which make the beam to focus downward toward the sample. SEM can magnify objects at maximum of 300,000 times the size of the object studied with 3-D image for researchers to analyze (Ezumi & Todokoro, 1999). High imaging speed and relatively high resolution of SEM make it a suitable characterization technique for nanostructures and their topographic features can be analyzed through it. The energy exhibited by secondary electron ranges around 10 keV that offer resolution at nanoscale and facilitate surface and size analysis in nanometres (Todokoro *et al.,* 2003).

In the present study, particle size and surface morphology of titania nanostructures were characterized by scanning electron microscope (JEOL JSM-6460) at an acceleration voltage of 20 kV. Also LDPE films were characterized with SEM for surface morphology and thickness analysis of pure LDPE and composite films before and after the irradiation exposure to observe any change due to photocatalytic degradation and see its relation to the weight reduction.

3.6.2 EDS Analysis

Energy Dispersive Spectroscopy (EDS) can provide elemental analysis or chemical composition of the sample on areas as small as nanometers in diameter. This analysis involves the generation of an X-ray spectrum from the entire scan area of the SEM and depends on interaction of X-ray source excitation and the sample (Ngo, 1999). When electron beam strike on a sample, inner shell electrons are excited, electron from outer shell fill that gap, energy difference is released in the form of X-rays which are characteristic of the elements present in the sample as shown in Figure 3.9. This property of characteristic X-ray lines allows sample elemental composition to be identified by a nondestructive technique. The elemental composition of individual points or mapping out of elemental lateral distribution from the imaged scan area can be obtained via EDS analysis (Wollman, 1997).
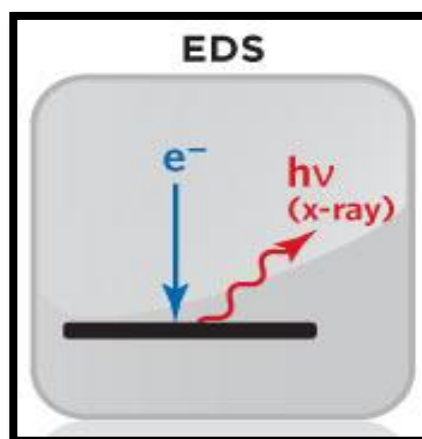
Fig 3.9 EDS working principle

In the present study, energy dispersive spectroscopic (EDS) spectra of TNPs and TNTs were obtained by using JEOL JSM 6490A analytical station to analyze the elemental composition.

3.6.3 X-Ray Diffraction Analysis

X-ray diffraction analysis relies on the dual wave/particle nature of X-rays and provides most definitive structural information of any powdered sample with interatomic distances and bond angle details. It is a well-established technique basically used for identification and characterization of compounds based on their diffraction pattern and for the quantification of the percent crystallinity of a sample (Zachariasen, 2004). In XRD, when an incident beam of monochromatic x-rays strikes on sample, scattering of those x-rays from atoms within the target sample occurs. The scattered x-rays undergo constructive and destructive interference in the regular crystalline materials. This is X-ray diffraction process as depicted in Figure 3.10. (Guinier, 1994). The size of crystallite size is determined by measuring the broadening of a particular peak in a diffraction pattern linked with a particular planar reflection from within the crystal unit cell (Chen and Mao, 2007).

If the experimental angle is systematically changed, all possible diffraction peaks from the powder will be detected. Diffraction of X-rays by crystals is described by Bragg's Law, $n\lambda = 2d \sin\theta$ (Gilmore, 2011). This law relates the wavelength of electromagnetic radiation to the diffraction angle and the lattice spacing in a crystalline sample. X-ray diffraction can indirectly reveal details of internal structure of the order of 10^{-10} m in size and due to this phenomenon it has wide application in the field of metallurgy (Authier, 2001).
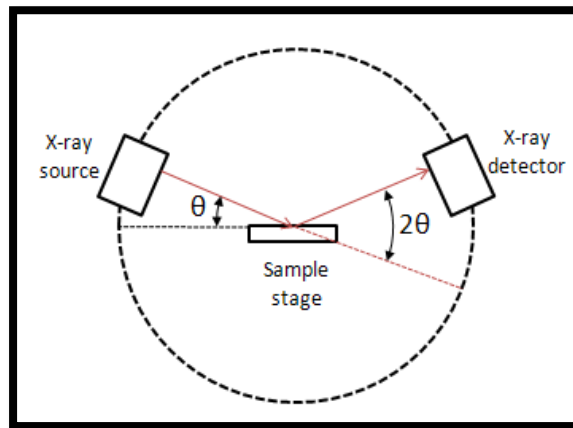
Fig 3.10. X-ray diffraction instrumentation

The crystallite size can be determined from the X-ray diffraction pattern, based on the Scherer formula: (Liu *et al.*, 2009).

$$L = \frac{k\lambda}{\beta \cos \theta}$$

Where,

k= 0.9, a shape factor for spherical particles

λ = 0.154056 nm, X-ray wavelength employed (CuKα1)

β= Full width of a diffraction line at one half of maximum intensity (FWHM) in radian

θ = the diffraction angle of the crystal plane (hkl)

In present Study, JEOL JDX-II X-ray diffractometer was used to analyze the crystalline phase of TNPs and TNTs.

3.6.4 Surface Area Measurements (BET)

Surface area and porosity are significant characteristics, capable of affecting the quality and utility of nanomaterials. The Brunauer, Emmett and Teller (BET) surface area

of a powder is determined by physical adsorption of surrounding gas on solid sample's surface and by calculating the amount of adsorbate gas. By measuring the amount of gas that is adsorbed in a monolayer, the surface area could be derived. The BET analyzer determine surface area at the temperature of liquid nitrogen (Brunauer *et al.,* 1938). Physical adsorption results from relatively weak van der Waals forces between the adsorbate gas molecules and the adsorbent surface area of the powder sample (Dogan *et al.,* 2006).

An Adsorption Isotherm is obtained by measuring the amount of gas adsorbed across relative pressures wide range at a constant temperature (Peigney *et al.,* 2001). The most important step before performing the test is to degas the sample in order to clean the sample of any organic vapors or moisture. In present study, Micromeritics Gemini VII BET surface area Analyzer was used to calculate the BET surface areas, Langmuir surface areas and pore diameter of titania nanoparticles and nanotubes. For BET analysis TNTs or TNPs samples were first degassed at 130 ºC for 4 h under vacuum (Akarsu *et al.,* 2006).

3.6.5 Weight loss measurements

Weighing is the determination of mass of an object using a balance with high precision. Analytical balances can measure weight down to thousandths or even hundred thousandths of a gram. It has doors to prevent air currents from interfering with the measurements. A butter paper is used to hold the LDPE film being weighed and protect the weighing pan. Analytical balance is tarred to subtract the weight of paper and make the scale re-zero so PE film can be accurately weighed.

In the present study, the weight loss of LDPE and composite films during photocatalytic degaration was measured with weighing balance of 0.0001 gm sensitivity

Schimadzu Model ATY-224 was used for weight measurements. The percentage mass loss was determined as follows.

$$\% \text{ Mass loss} = \frac{mi - mf}{mi} \text{x } 100$$

Where

m_i = Initial weight before irradiation

m_f = Final weight after irradiation

The purpose of the weight reduction measurements was to have an indirect measure of photo catalytic degradation of pure PE and PE-TNPs or PE-TNTs composite films during irradiation time.

3.6.6 Surface Roughness Measurement

Surface roughness is a component of surface texture. There are two ways to measure surface roughness either mechanically or optically. The use of mechanical devices which are equipped with profilometric principles are expensive, unreliable in certain specific purposes and require physical contact with sample which further damage the sample's surface and can corrupt the measurement data. On the other hand, noncontact optical profilometers resolve the issues of surface damage and measurement data but it needs optical devices with high accuracy and must be realigned continually (Meeks & Kudinar, 2002).

Profilometric analysis have many applications in material science to examine the surface morphology or irregularities. Surface roughness is directly assessed by measuring the valleys and peaks on material surface. Contact profilometer measures rougness upto micrometer range (Lee & Cho *et al.,* 2012). In optical profilometer, a sharp needle is mounted on a cantilever that moves along a line on material's surface and records all

displacements induced by surface irregularities. A transducer is used for amplification of displacements recording into electric signals (Tawashi *et al.,* 1994). For vertical displacements measurement, a photoelectric cell is used which amplifies and appears all signals directly on monitor attached with profilometer analyzer (Chappard *et al.,* 2003).
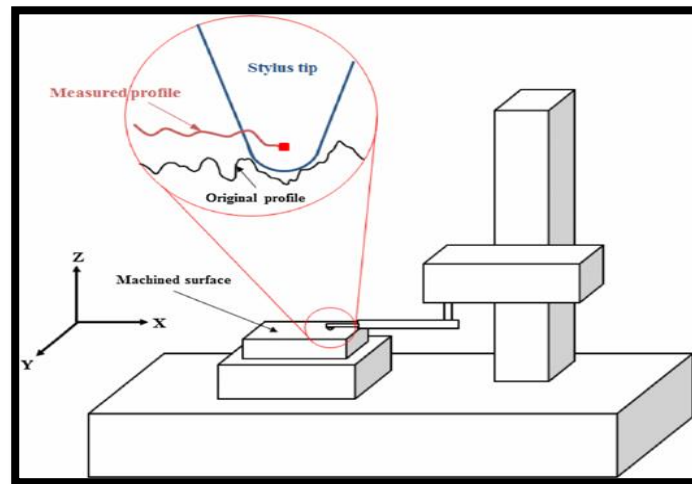
Fig 3.11 Surface irregularities recorded by a transducer in optical profilometer (Lee and Cho *et al.,* 2012)

For 2D characterization of surface roughness, parameters such as R_a, R_z, S, and S_m are commonly used in national standards (Myshkin *et al.,* 2003). For a given specimen, several test lines need to be measured and averaged. SEM is also helpful for qualitative study of surface topography but this is just limited to morphological approach of roughness. But profilometer is used to measure a surface's profile, in order to quantify its roughness (Chappard *et al.,* 2003).

The high-performance PS50 with 50mm X-Y stages, is the ideal choice to replace stylus and laser profilers. In the present study, Nanovea 2d Optical profilometer PS50 was used to measure the surface roughness of polyethylene films before and after irradiation.

3.6.7 FTIR analysis

Fourier transform infra-red spectroscopy (FTIR) is one of excellent tool for identification of unknown compounds and it provides information about chemical structure of those molecules within the compounds. Fourier transform is required to convert the raw data into the actual spectrum. When infrared rays are passed through the compound, chemical structure of molecules inside that compound can be known by absorbing specific wavelengths of the infrared spectrum unique to that compound and vibrations of that molecular species. Because each different material is a unique combination of atoms, no two compounds produce the exact same infrared spectrum (Gulmine *et al.,* 2002).

Those wavelengths which are not absorbed pass through to the detector and an absorbance pattern is made which is further compared with the library database for identification of compounds. The infrared spectrum can be obtained by plotting absorbance or percent transmittance against frequency or wavelength and ranges from 4000 to 450 cm^{-1}. Two unique molecular structures cannot produce the same infrared spectrum just like fingerprint. This makes infrared spectroscopy useful for several types of analysis (Rajandas *et al.,* 2012).

An FTIR is usually based on the Michelson Interferometer Experimental Setup and it has 5 basic components as shown in Figure 3.12.

- The source
- The interferometer
- The sample
- The detector
- The computer
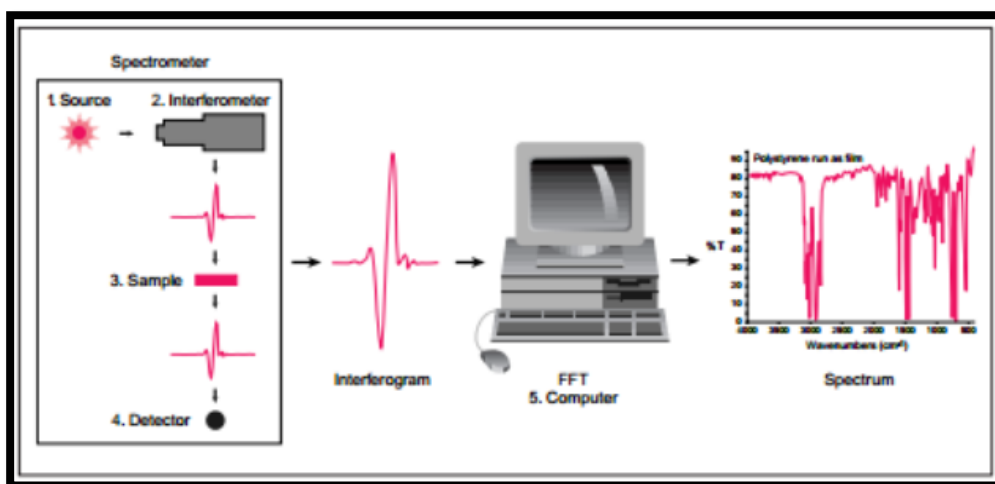
Fig 3.12 FTIR Working and set up

In case of degradation of polymers, FTIR is the most commonly used technique to find out the chemical structure of molecules inside the LDPE matrix and result in a positive identification of every different kind of material. It detects carbonyl groups formation after oxidation and incorporation of oxygen into polyethylene's chemical structure (Dilaraa & Briassoulis, 1998).

FTIR has great sensitivity for the gaseous products H_2O, CO_2 and carboxylic acids in the polymer matrix (Chiellini *et al.*, 2003). In present study FTIR spectra of PE and composite films were obtained using Perkin Elmer Spectrum FTIR spectrometer. Degradation rates were calculated by using the standard carbonyl index method. The comparison study was carried out in order to find out information about the carbonyl groups.

3.6.8 Mechanical testing

Tensile strength testing is one of those methods which is used to measure strength of any material which are used in structural applications. It gives the values of the ability of any material to withstand force per unit area (MPa) which tends to pull apart that material. It is the ultimate tensile strength or the tensile strength at break. It helps to

determine the extent at which material can be stretched before breaking (Tay & Teoh, 1989). The test geometry is as shown in Figure 3.13(a).
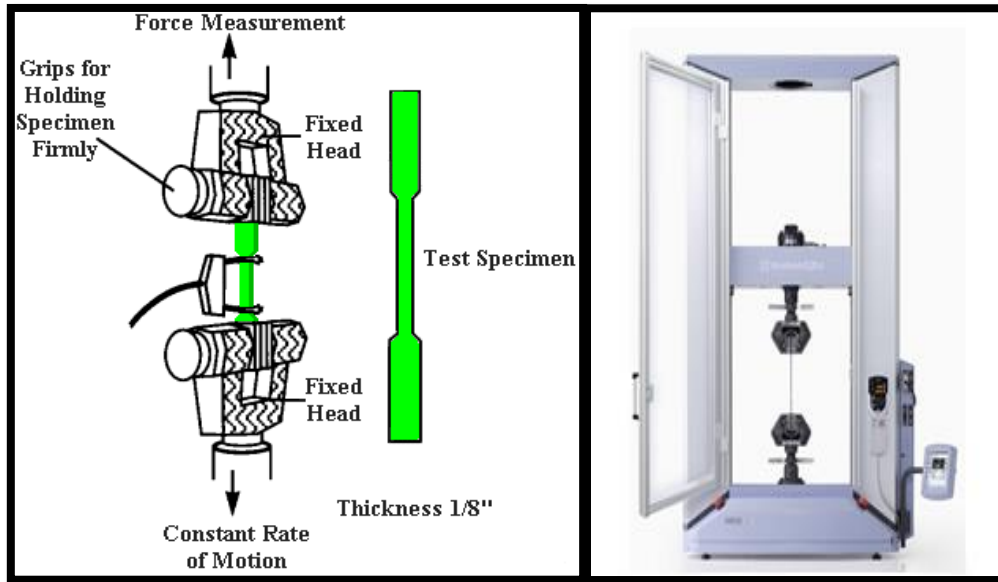
Fig 3.13. a) Tensile strength test geometry b) External view of Schimadzu testing machine

Pulling rate of sample can vary from 0.2 to 20 inches (0.508 to 508 mm) per minute which also effects the final results. The second important parameter is elongation of a polymer which is the percentage increase in length that occurs before it breaks under tension (Powell & Housz, 1998). The method ASTM D 882 established by American Society for Testing and Materials (ASTM) is well suited for films less than 0.25 mm and that method is followed in our present study.

In this protocol, the specific strips having uniform thickness and width with having specific provisions like special grips to prevent slippage and breakage of LDPE specimens are employed. LDPE has relatively low tensile strength in range of 4.1 – 15.9 MPa (Konduri *et al.,* 2011). Reduction in tensile strength is used as standard method to indicate degradation of Polyethylene.

In the current study, tensile testing was done to determine the strength of Polyethylene films. Universal Testing machine (Schimadzu AG XPlus 20kN) was used for this testing. Samples with a gauge length of 30 mm and width of 10 mm were cut from the films and run at speed of 1mm/min for tensile strength measurements. All tests were performed at room temperature. The average values of the tensile strength and percentage of elongation were determined. Tensile strength is calculated by this formula and final results are expressed in Megapascals (MPa) (Jancar, 1999).

$$\text{Tensile Strength} = \frac{\text{load at break}}{\text{original width x original thickness}}$$

Percent elongation is measured by this formula.

$$\% \text{ Elongation} = \frac{\text{Elongation at rupture x100}}{\text{Initial guage length}}$$

RESULTS AND DISCUSSION

4.1 SEM Analysis of Nanostructures

Figure 4.1 & 4.2 show the morphology and diameters of pure TNPs measured by scanning electron microscope at 20,000 and 40,000 magnifications. The diameter of spherical particles ranges from 39 to 80 nm with an average value of 50 nm. Figure 4.3 & 4.4 show the morphology and diameters of pure TNTs taken by SEM at 20,000 and 30,000 magnifications. The average diameter of nanotubes is 40 nm and range from 18 nm to 58 nm. A large amount of randomly tangled TNTs are produced which are in the form of clusters and not completely separated from each other. Due to their tubular structure TNTs exhibit greater surface area as compared to nanoparticles. These images shows that the size of nanoparticles and nanotubes are good enough to use in our experiments to carry photocatalytic activity.
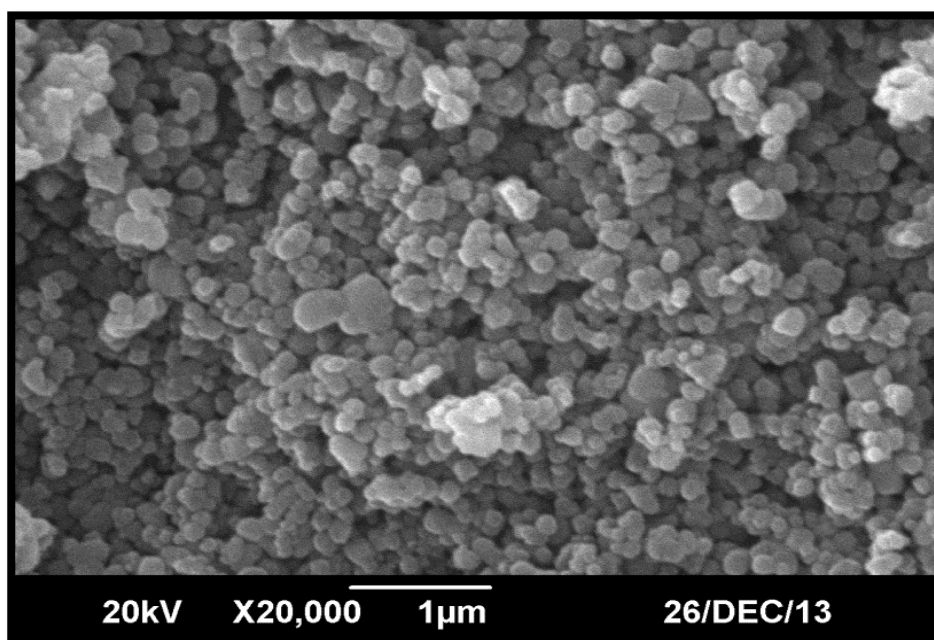
Figure 4.1 SEM image of TNPs at X20, 000
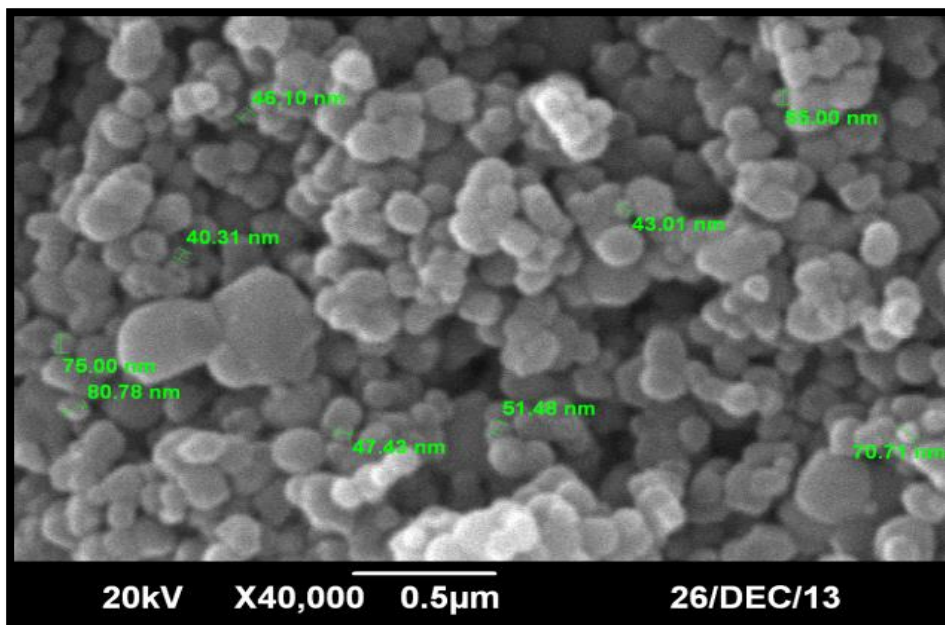
Figure 4.2 SEM image of TNPs at X40, 000
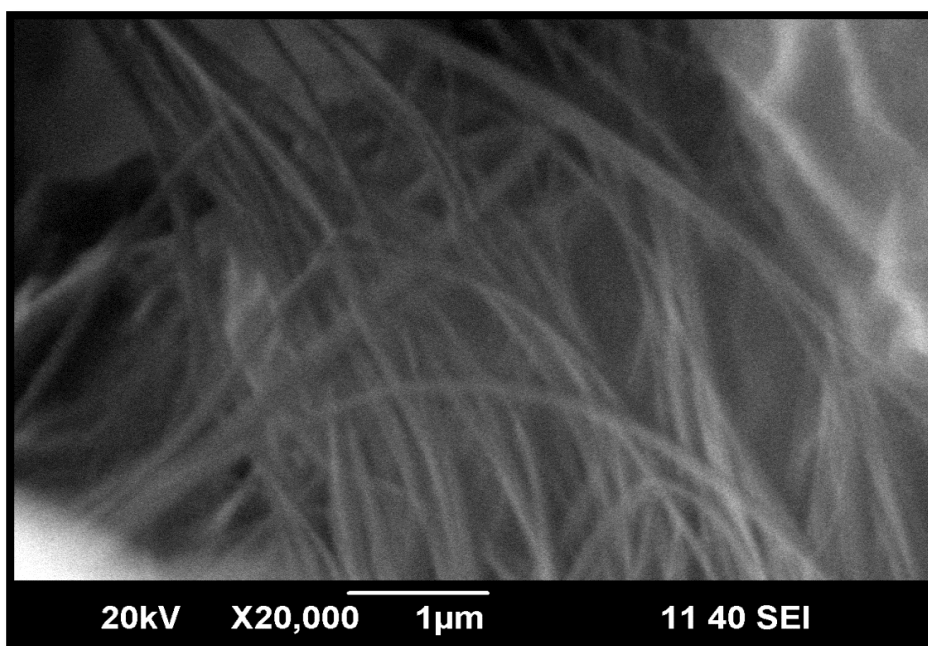
Figure 4.3 SEM image of pure TNTs at X20, 000
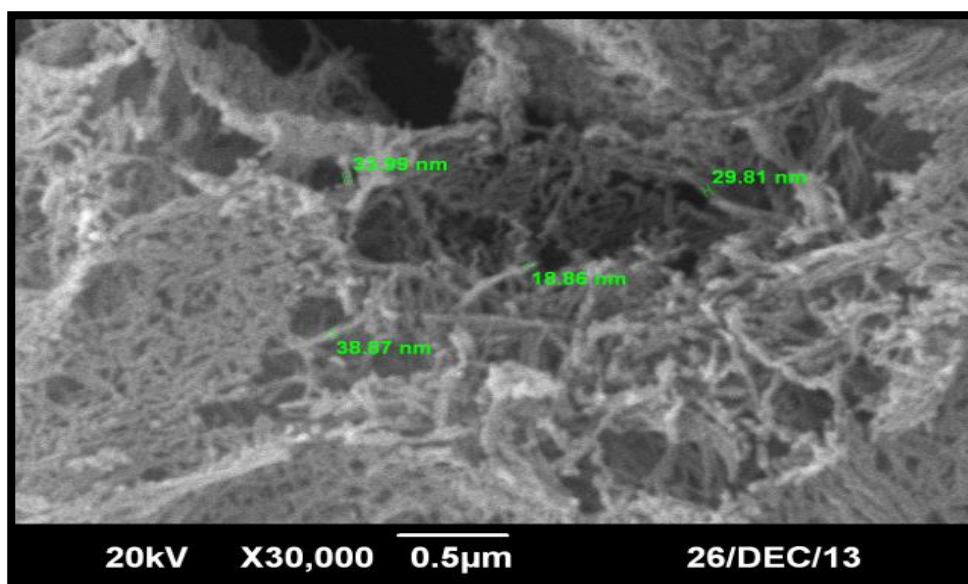
Figure 4.4 SEM image of pure TNTs at X30, 000

4.2 EDS analysis

EDS analysis was done to get elemental composition of nanostructures. EDS graphs are shown in Figure 4.5 and 4.6 for TNPs and TNTs respectively. The EDS analysis of an area containing a large amount of tubular particles reveal the existence of Na, Ti and O elements.
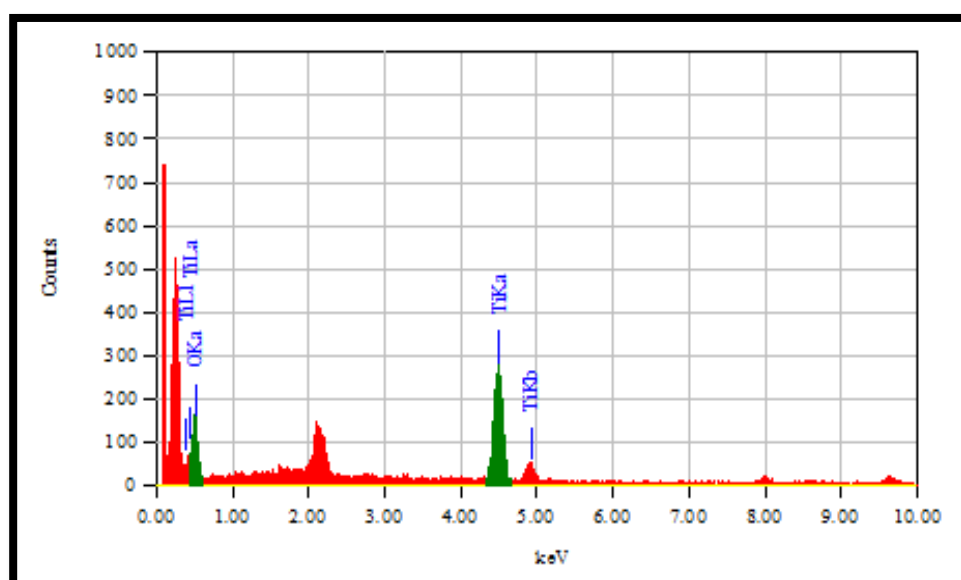
Figure 4.5 Elemental Composition of pure TNPs

The mass percentages of elements are tabulated in Tables 4.1 and 4.2.

Table 4.1 Mass % of elements in pure TNPs

Element	Mass percent	
	Experimental	Expected
Ti	56%	60%
O	44%	40%

The major constituents for pure TNPs and TNTs are Titanium and Oxygen i.e. approximately 56% and 44% in TNPs and 57% and 41% in TNTs respectively indicating the sample to be pure. Na and Ca peaks (2%) are also observed there which are due to NaOH and water used during nanotubes synthesis and washing process.
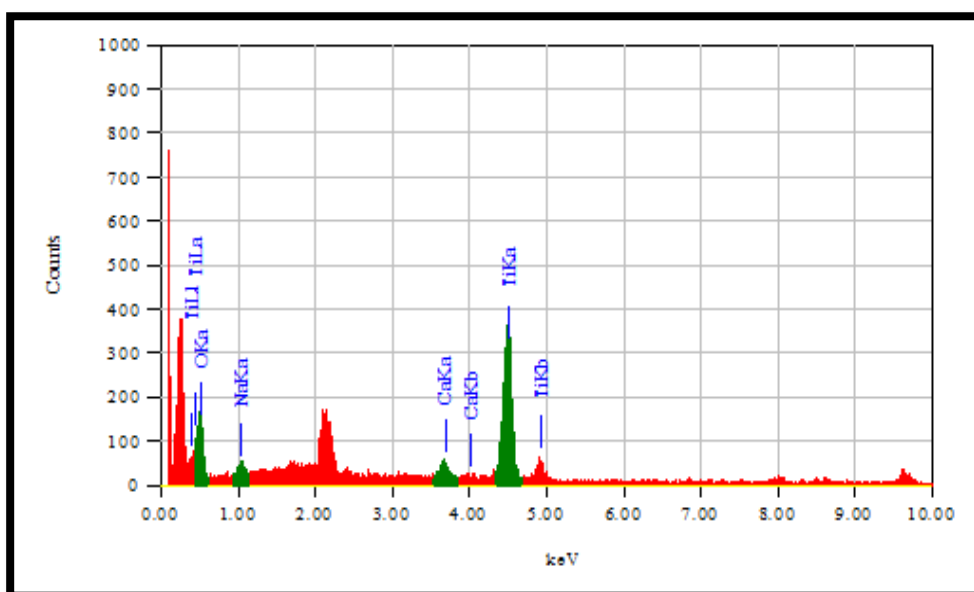
Figure 4.6 Elemental composition of pure TNTs

Table 4.2 Mass % of elements in pure TNTs

Element	Mass percent	
	Experimental	Expected
Ti	57%	60%
O	41%	40%

4.3 XRD analysis

XRD analysis of nanostructures was carried out to determine their crystallinity, polymorph phase and composition. XRD graphs are obtained by powder XRD technique using Cu-Kα radiations at an angle of 2θ from 10° to 80° with a scanning step size of 0.021^o. Figure 4.7 shows the XRD results of nanoparticles where 2θ peaks at 25.30(100), 36.95(6.1), 37.79(18.6), 48.04(24.2), 55.07(14.8) are visible. The presence of four main peaks at 2θ values of 25.3^o, 36.9^o, 48.04^o and 55.07^o represents that TNPs are typical of anatase phase of TiO_2. Thus, the existence of rutile phase is not observed.
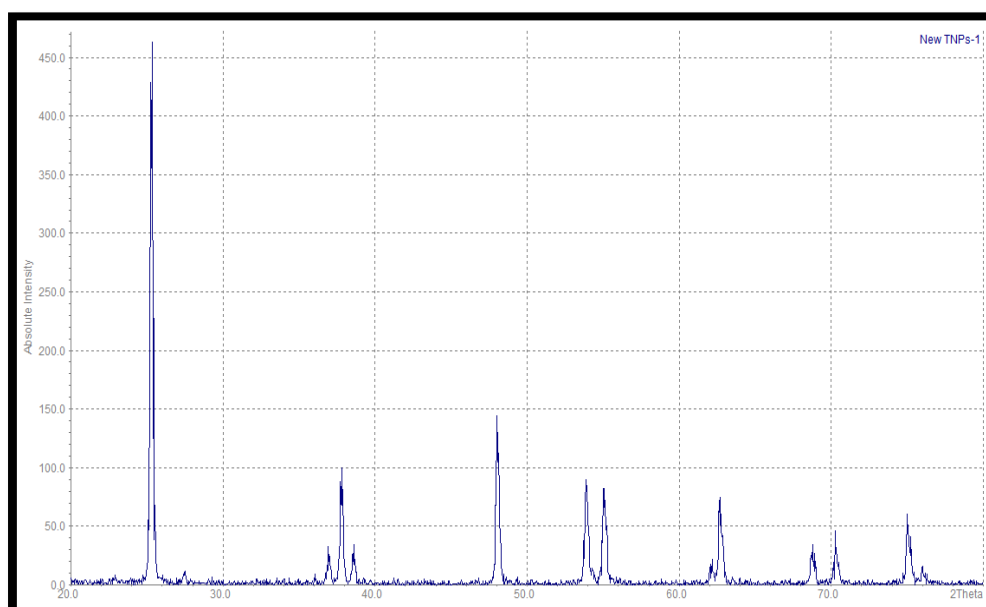
Fig 4.7 XRD Intensity plot for pure titania nanoparticles

Figure 4.8 shows the XRD pattern of titania nanotubes. The diffraction peaks at about $2\theta=$ 25°, 38°, 48°, 55°, 56° and 63° can be indexed to the (101), (103), (004), (200), (105), and (211) planes of the anatase crystalline phase of Titania Nanotubes. These diffraction peaks are all enhanced by the increased length of nanotube arrays. The diffraction patterns of titania nanotubes shows some increase in the intensity of anatase peaks. All these peaks are revealing that synthesized TNPs and TNTs are highly crystalline in nature and are upto 80% anatase.
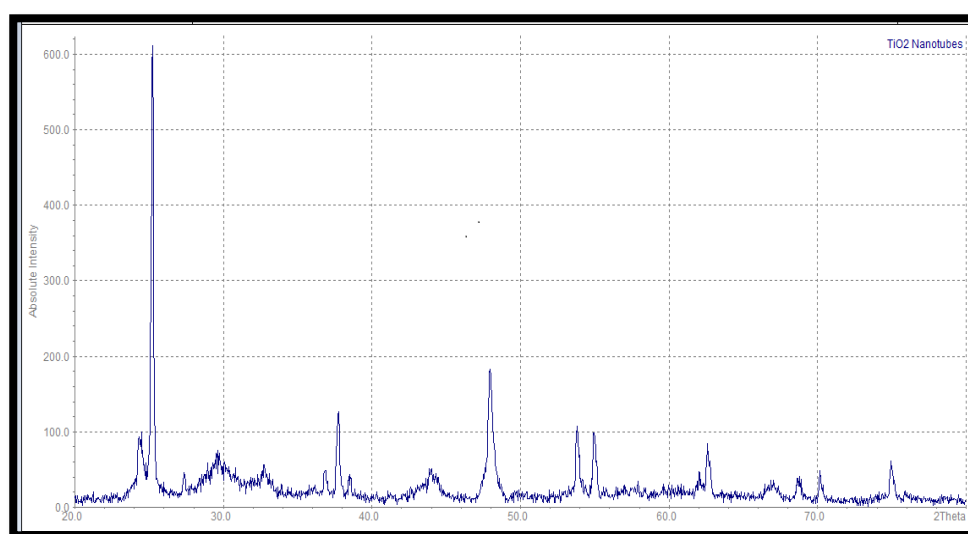
Fig 4.8 XRD Intensity plots of Titania nanotubes

Anatase has a higher photocatalytic activity than rutile because anatase has a larger band-gap than rutile, 3.2 eV versus 3.0 eV, respectively. Anatase phase is chemically stable at calcination temprature >700 °C and is suitable for use as a catalyst (Fen *et al.,* 2011). Higher calcination temperature results in the stronger diffraction peak, which shows that higher temperature required for the formation of titania anatase in the range of 300 – 500 °C (Wang *et al.,* 2008). Achieving anatase phase in higher percent is a temperature dependent process (Sayilkan *et al.,* 2005). The phase structure and composition, crystallite size and crystallinity of TiO_2 are of great influence on its photocatalytic activity and photoelectrochemical properties (Yu *et al.,* 2003).

Calcination temperatures have impact on the crystallization and phase structures of the TNTs samples. Average crystalline sizes and anatase crystallinity increases with increasing calcination temperatures (Yu *et al.,* 2010). The TNTs should be calcined at 450 °C for 2 h, which would make good crystalline structure and larger surface area (Xiao *et al.,* 2010). But increasing temperature above 600°C causes nanotubes collapse into nanoparticles, suggesting the occurrence of phase transformation of anatase to rutile (Yu *et al.,* 2009; Lee *et al.,* 2011).

4.4 BET Analysis

Specific surface area and pore volume of the TNPs and TNTs were determined using the BET method based on N_2 adsorption/desorption isotherm at 77 K. The specific surface area values are shown in Table 4.3. BET analysis of pure TNPs and TNTs revealed that at a relative pressure of 0.25 maximum amount of liquid Nitrogen adsorbed on the surface of nanoparticles is about 25 cm^3/g at Standard Temperature & Pressure (STP) as shown in Figure 4.9. And maximum amount of liquid Nitrogen adsorbed on the surface of nanotubes is about 48 cm^3/g as shown in Figure 4.10.
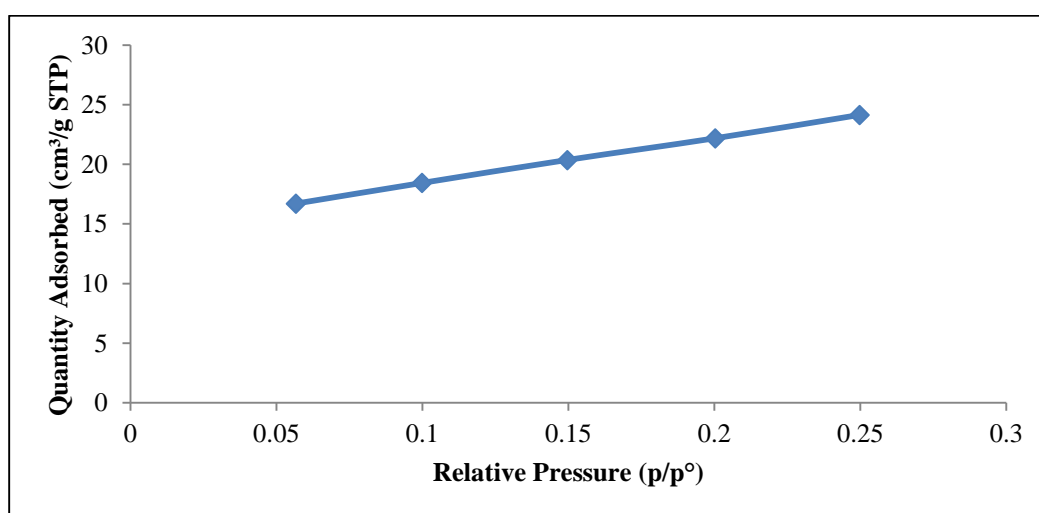
Fig 4.9 Isotherm Linear Plot for N_2 Adsorption (Pure TNPs) at 77K

This refers to almost 81 m^2/g surface area of pure TNPs and 161 m^2/g for nanotubes, matching with the surface area limits for such nanostructures. It can be seen

that the specific surface area of the nanostructures before hydrothermal treatment (81 m^2/g) increases to 161 m^2/g after treatment.
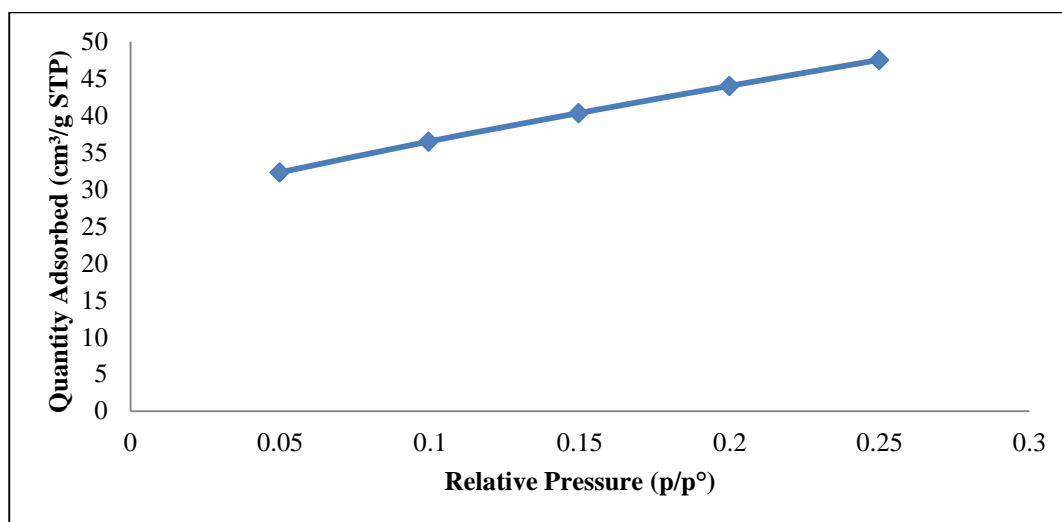
Fig 4.10 Isotherm Linear Plot for N_2 Adsorption (Pure TNTs) at 77K

Table 4.3 shows the BET surface area, pore size and pore volume of all the TiO_2 nanostructures.

Sample	BET surface area (m^2/g)	Pore Size (Å)	Pore volume (cm^3/g)
Pure nanoparticles	81	18.322	0.028365
Pure nanotubes	161	18.330	0.101829

Table 4.3 Comparison of BET analysis of nanostructures

4.5 Photocatalytic Degradation Experiments

4.5.1 Weight loss measurements

LDPE film weight reduction measurement was carried out to study their photo-degradation. Figure 4.11 and 4.12 displays the photo induced weight loss of different samples with visible light using nanoparticles and nanotubes respectively. The values of

'k$'$' for each titania nanostructures concentration (0 to 15%), values of the *Correlation Coefficient* 'R^2' and half-life of each composite are tabulated in Table 4.4 and 4.5. Weight loss data was plotted again time (d) and exponential equation was fitted on it as first order kinetics

$$dW/dt = -kt \qquad [Eq. 1]$$

Here 'k' is the '*degradation rate constant*' and, with W$_o$ is the weight at day '0', the start of the disintegration process, integration of the equation leads to Equation 2.

$$W = W_o e^{kt} \qquad [Eq. 2]$$

Figures 4.13 and 4.14 display the photo induced weight loss of different samples with UV light using nanoparticles and nanotubes respectively.
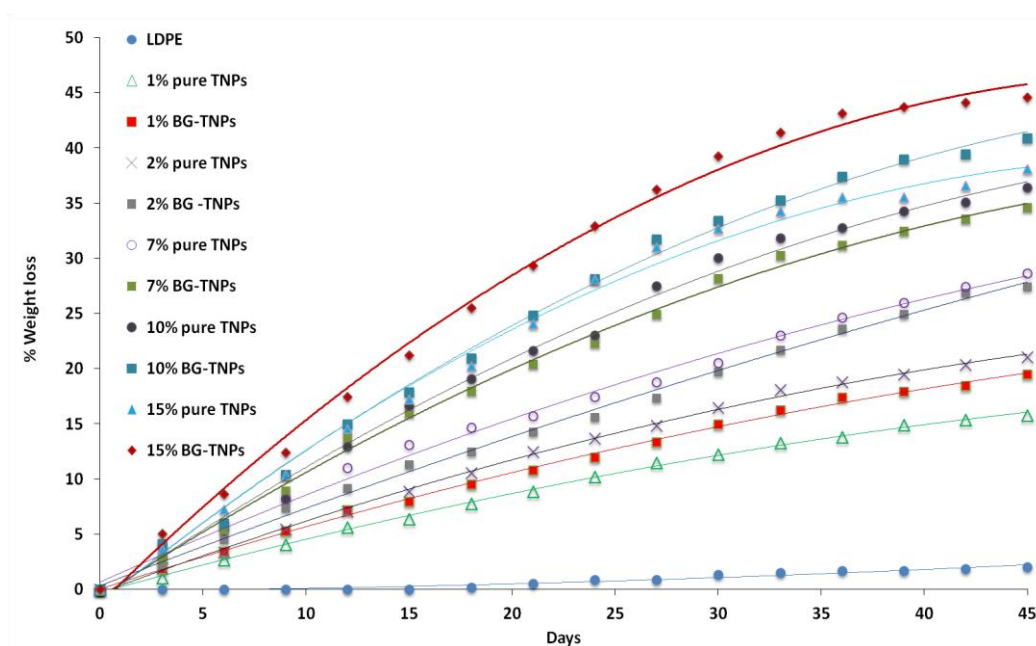
Fig 4.11 Weight loss of LDPE-TNPs composite films after visible light irradiation for 45 days
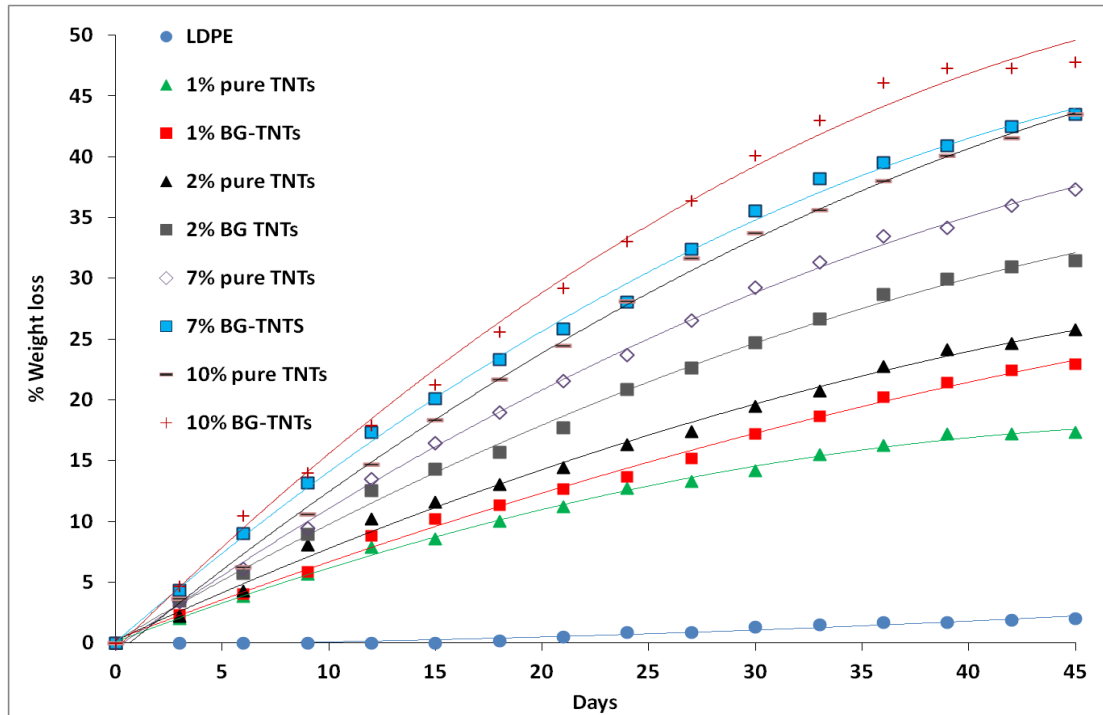
Fig 4.12 Weight loss of LDPE-TNTs composite films after visible light

irradiation for 45 days
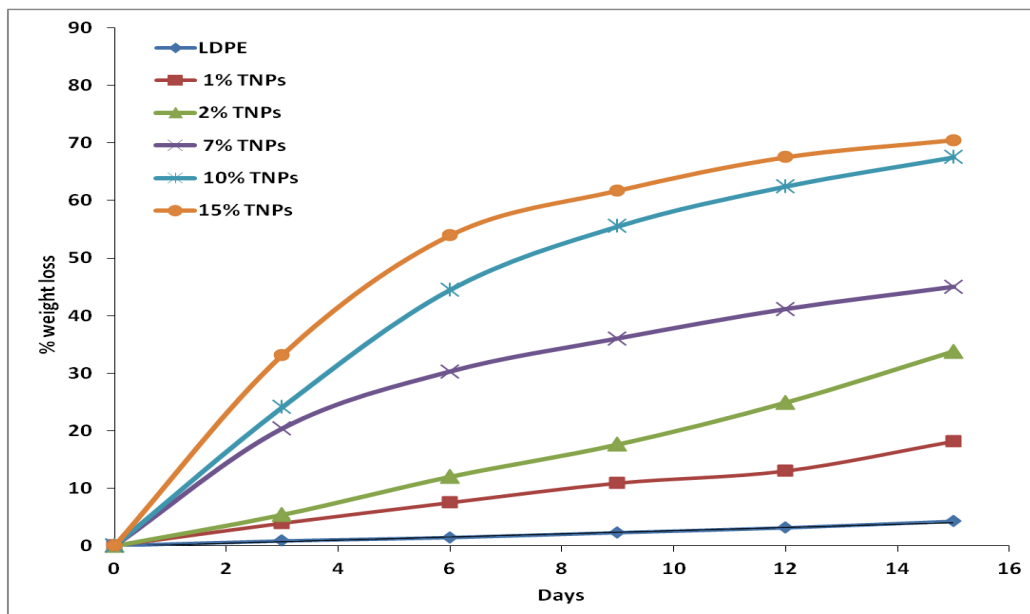
Fig 4.13 Weight loss of LDPE-TNPs composite films after UV light irradiation
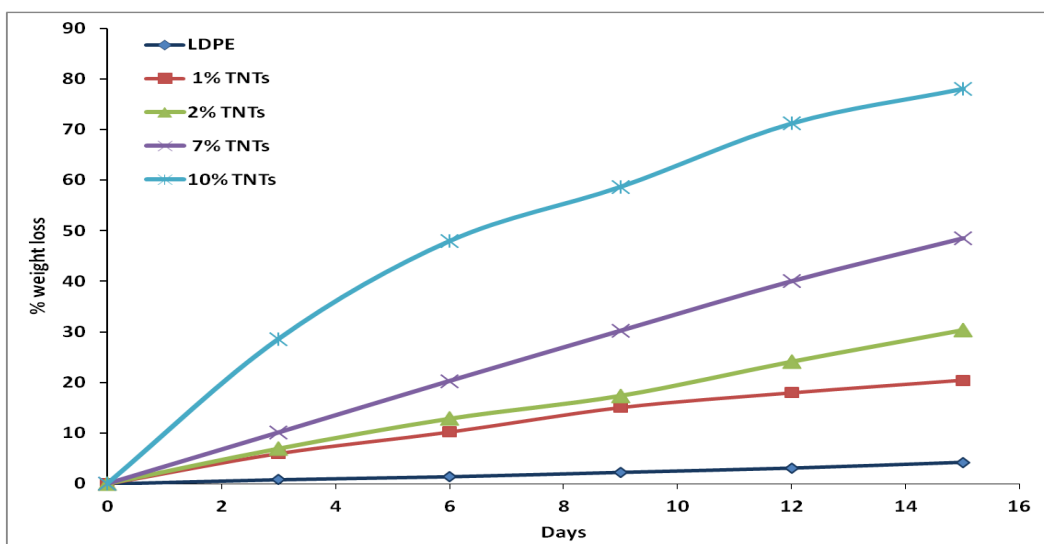
for 15 days

Fig 4.14 Weight loss of LDPE-TNTs composite films after UV light

irradiation for 15 days

Pure LDPE films showed no noticeable weight loss after irradiation but TNPs embedding in LDPE matrix lead to noticeable weight loss of films. Also, the weight loss rate for those LDPE films which contain brilliant green (BG) dye sensitized TNPs is higher than PE films containing pure TNPs as shown in Figure 4.11. Similarly, composite films containing TNTs or BG sensitized TNTs showed faster degradation rate under visible or UV light than TNPs. Composite films containing TNTs or BG sensitized TNTs showed higher degradation rate as compare to nanoparticles which goes maximum upto 48% under visible light. Hence, dye sensitized nanotubes showed effective photo degradation of LDPE.

Polyethylene films degraded very fast under UV light because organic chains of LDPE are likely to be broken by the UV radiation. Figure 4.15 displays the photo induced weight loss of different samples under UV using nanoparticles and nanotubes from 1 to 10% ratio by weight of polythene. Pure LDPE films showed 4% weight loss after UV exposure but nanostructures embedding in films leads to the weight loss of films

and showed maximum degradation upto 67% in case of nanoparticles and 78% in case of 10% Titania nanotubes.
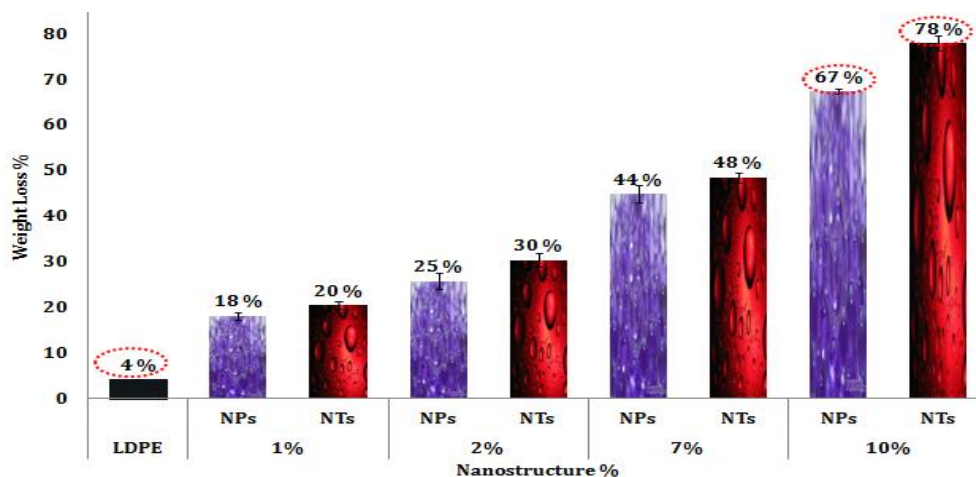
Fig 4.15 Comparison between NPs and NTs composites weight loss after UV light

irradiation
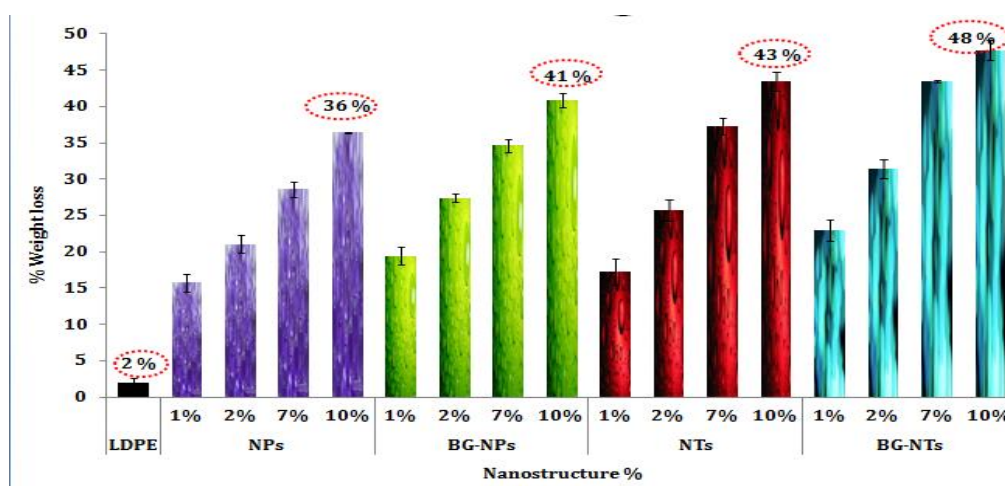
Fig 4.16 Comparison between NPs, NTs and dye sensitized nanostructures

composites weight loss after visible light irradiation

Negligible weight reduction was recorded for the pure LDPE film and all the composite films with TNPs and TNTs during 45 days under dark conditions which reveals that pure LDPE and composite films remained stable and no degradation to any extent occurred under no irradiation conditions.

Table 4.4 Weight loss data (under UV for 15 days) after applying Exponential Equation

		W_o (gm)	K	R^2	$\lambda_{1/2}$ (d)
Titania Concentration in Percentage (w/w)	0%	0.0176	0.0003	0.9912	2310
	1% TNPs	0.0205	0.001	0.9913	693
	2% TNPs	0.0191	0.002	0.989	346
	7% TNPs	0.0216	0.004	0.8952	173
	10% TNPs	0.0198	0.004	0.9194	173
	15% TNPs	0.0150	0.005	0.8239	138.
	1% TNTs	0.0184	0.001	0.9696	693
	2% TNTs	0.0197	0.003	0.914	231
	7% TNTs	0.0229	0.005	0.922	138
	10% TNTs	0.0196	0.006	0.994	115

Table 4.5 Weight loss data (under visible light for 45 days) after applying Exponential Equation

		W_o (g)	K	R^2	$\lambda_{1/2}$ (d)
Titania Concentration in Percentage (w/w)	0%	0.0150	0.00009	0.593	7700
	1% TNPs	0.0201	0.0009	0.8738	770
	2% TNPs	0.0172	0.001	0.8774	693
	7% TNPs	0.0171	0.001	0.8895	693
	10% TNPs	0.0194	0.002	0.8823	346
	15% TNPs	0.0195	0.002	0.8815	346
	1% BGTNPs	0.0197	0.001	0.8728	693
	2% BGTNPs	0.0113	0.001	0.8576	693
	7% BGTNPs	0.0204	0.002	0.8872	346
	10% BGTNPs	0.0204	0.003	0.8818	231
	15% BGTNPs	0.0229	0.003	0.8937	231
	1% TNTs	0.0187	0.001	0.8855	693
	2% TNTs	0.0184	0.001	0.8898	693
	7% TNTs	0.0221	0.002	0.8833	346
	10% TNTs	0.0205	0.003	0.8752	231
	1% BGTNTs	0.0194	0.001	0.8663	693
	2% BGTNTs	0.0197	0.002	0.8849	346
	7% BGTNTs	0.0194	0.002	0.899	346
	10% BGTNTs	0.0197	0.004	0.8815	173

Pure LDPE can degrade up to its half weight in 2310 days but addition of 10% TNPs can make it to degrade in 173 days and 115 days with 1% TNTs. Similarly under visible light, half-life of pure LDPE is 7700 days which modified up to 173 days by adding 10 % titania nanotubes.

4.5.1.1 Comparison with previous study at IESE

Asghar *et al.,* 2011 had used doped and undoped TNPs for photocatalytic degradation of PE films. In that study, 1% by wt TNPs were used in composite films and irradiation time was 300 h. Brief summary of the photocatalyzed weight reduction (maximum) of pure PE film and PE-TiO$_2$ films is given below in Table 4.6.

Table 4.6 Weight loss data (for 300 h)

Sample		Maximum Weight Reduction (%)	
		UV Irradiation	Visible Light
1	**Pure PE**	3.32	0.65
2	**PE + TiO$_2$**	10.6	6.51

Now in current study, TNPs (1 to 15% by weight) and TNTs (1 to 10% by weight) are used to degrade LDPE. Increased light intensity of (2.54 mW/cm^2 was used in this study as compare to previous study (1.4 mW/cm^2). Irradiation time is also increased till 15 days in case of UV light and 45 days for visible light. In results, same pattern of degradation rate was observed in case of 1% TNPs under both UV and visible light and degradation rate was continuously enhanced with increasing nanostructures dosage. TNTs showed more degradation rate than nanoparticles in same time of irradiation.

4.6 Tensile Strength Measurements

Tensile testing was done to determine the strength of LDPE films. The testing procedure was followed according to ASTM 882-85 with using universal testing machine (Schimadzu AG XPlus 20kN). Samples with a gauge length of 30 mm and

width of 10 mm were cut from the films and run at speed of 1mm/min for tensile strength measurements. The average value was presented for each sample. Addition of nanostructure modifies the mechanical properties of LDPE composites which can be seen from their elongation at break (ε_b) average values for each sample as reported in Table 4.7. Tensile strength is calculated by this formula and final results are expressed in Megapascals (MPa).

$$\text{Tensile Strength} = \frac{\text{load at break}}{\text{original width x original thickness}}$$

Percent elongation is measured by this formula.

$$\% \text{ Elongation} = \frac{\text{Elongation at rupture x100}}{\text{Initial gage length}}$$

Table 4.7 Tensile strength and Elongation values for pure and composite films before and after irradiation

Sample Composition	Tensile Stength (MPa)		Break Elongation (%)	
	Before	After	Before	After
Pure LDPE	10.2	9.8	3.53	3.41
LDPE+2%TNPs	8.88	3.37	7.31	3.19
LDPE+7%TNPs	8.37	0.92	3.12	1.95
LDPE+2%TNTs	14.7	2.17	7.37	1.52
LDPE+7%TNTs	8.81	1.84	7.12	1.73

From their tensile strength and break elongation it can be interpreted that films degradation has a negative effect on the tensile strength of films. Addition of nanostructures also effect tensile properties of LDPE films as density of LDPE increases, tensile strength increases while elongation percent decreases. The high percentage of TNPs or TNTs causes agglomeration in LDPE and ultimately cause loss of tensile

strength as nanostructures agglomeration in LDPE matrix cause some morphological alterations (Fa *et al.,* 2010). Elongation also correlate with the formation of carbonyl groups because during degradation as carbonyl ratio increases, percent elongation decreases (Dilara & Briassoulis, 2000). The LDPE-TNTs composite films show evidence of much higher ε_b than pure LDPE film. LDPE films containing 7% titania nanostructures showed maximum elongation loss and tensile strength decline after 45 days of irradiation. The films degraded after UV radiation broke down on touching and were so fragile that tensile testing could not be performed on these films.

4.7 SEM Analysis

SEM images of LDPE and different composite films after irradiation at 5000 to 5500 magnifications are shown in Figures 4.18 (a,b,c,d,e,f,g). The surfaces of those polyethylene films which contain BG sensitized TNPs or TNTs (c & f) are more damaged than simple LDPE films containing pure TNPs or TNTs (b & e). These composite films showed some cavities from degradation with large interconnected holes. Formation of volatile degradation products might have produced such cavities in films (Liu *et al.,* 2009). These results proved that degradation efficiency of BG-TNTs is much better than TNPs under visible light irradiation. This result is according to weight loss values shown in Figures 4.11 & 4.12. Figure 4.17 shows the thickness analysis results of the LDPE-TNTs composite films before and after degradation under visible light for 45 days as after the degradation the thickness has increased double possibly due to the release of volatile organic compounds like CO_2 causing swelling of the LDPE films.
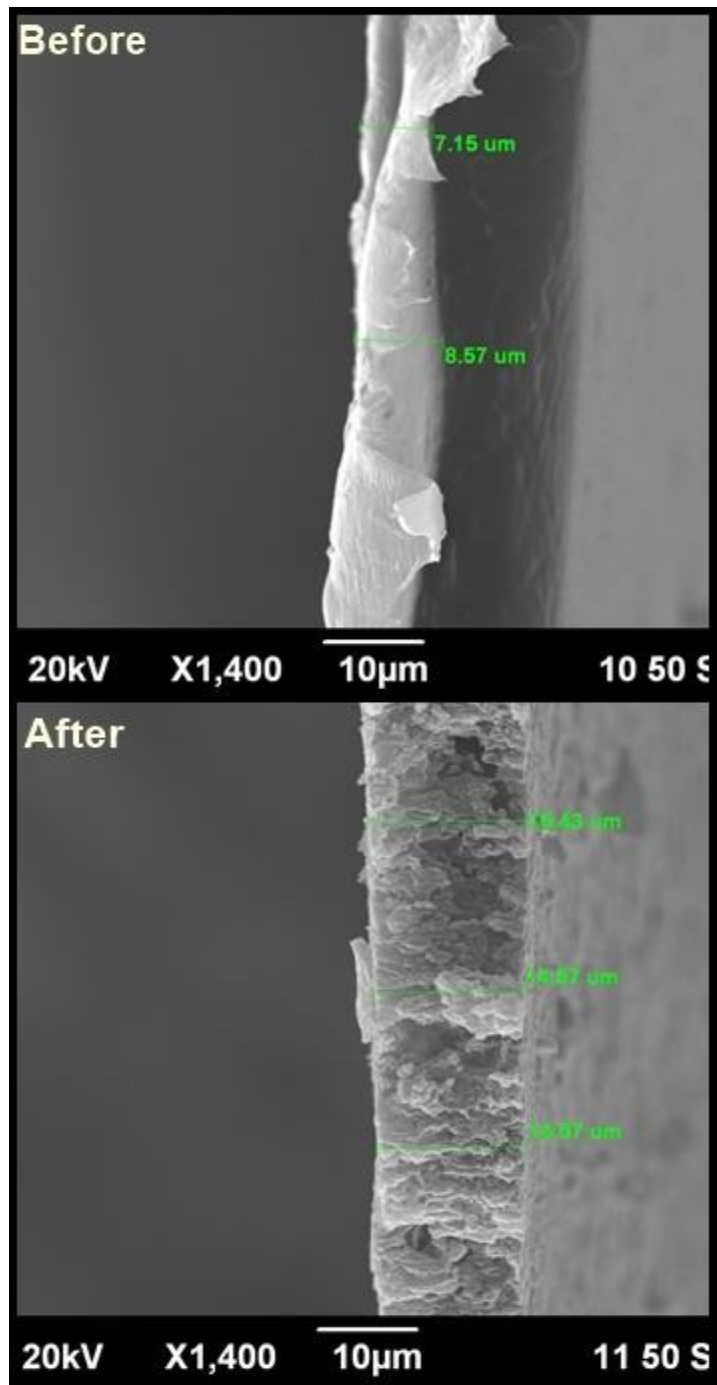
Fig 4.17 LDPE Composite films containing 2% TNTs before and after visible light irradiation for 45 Days
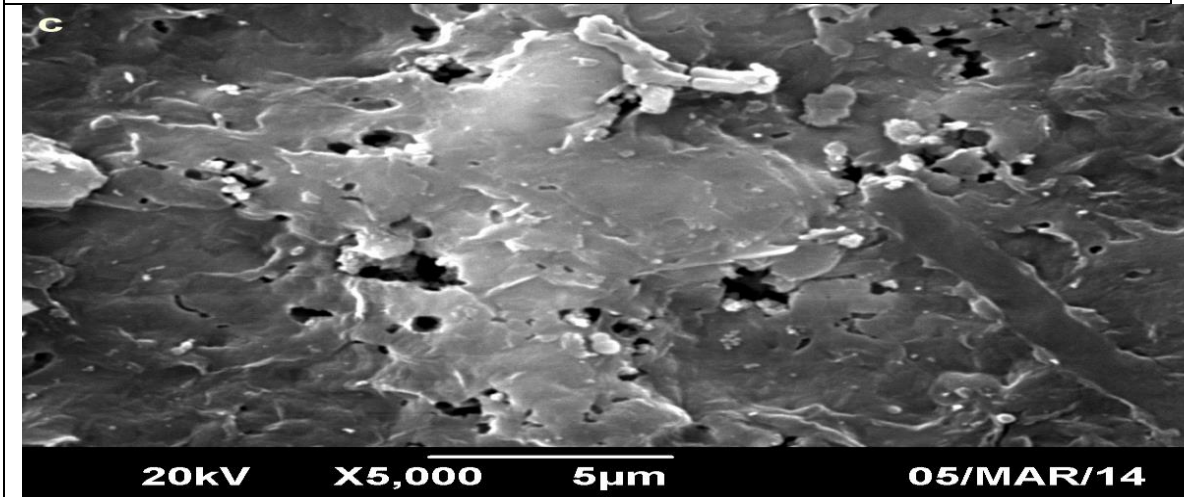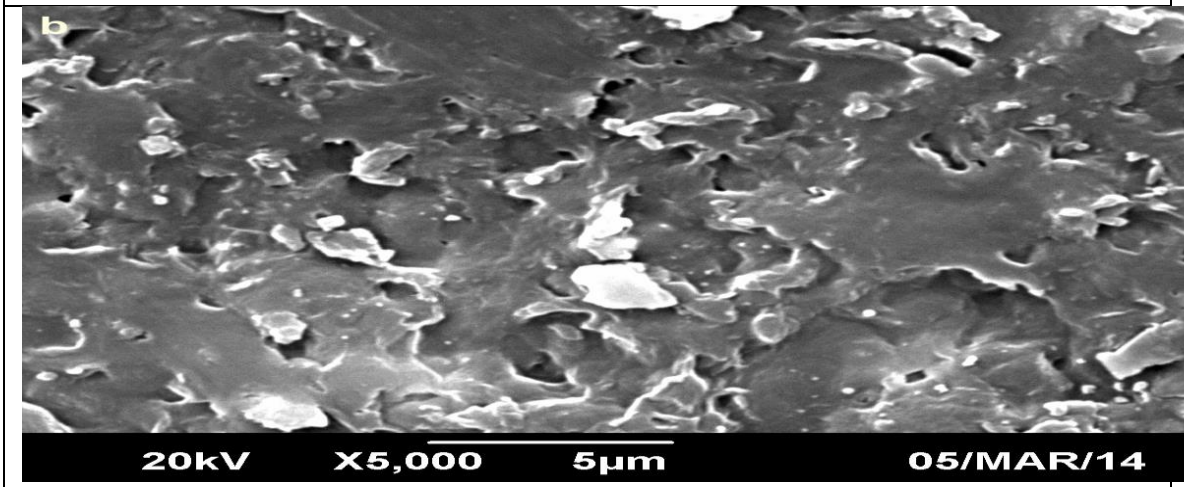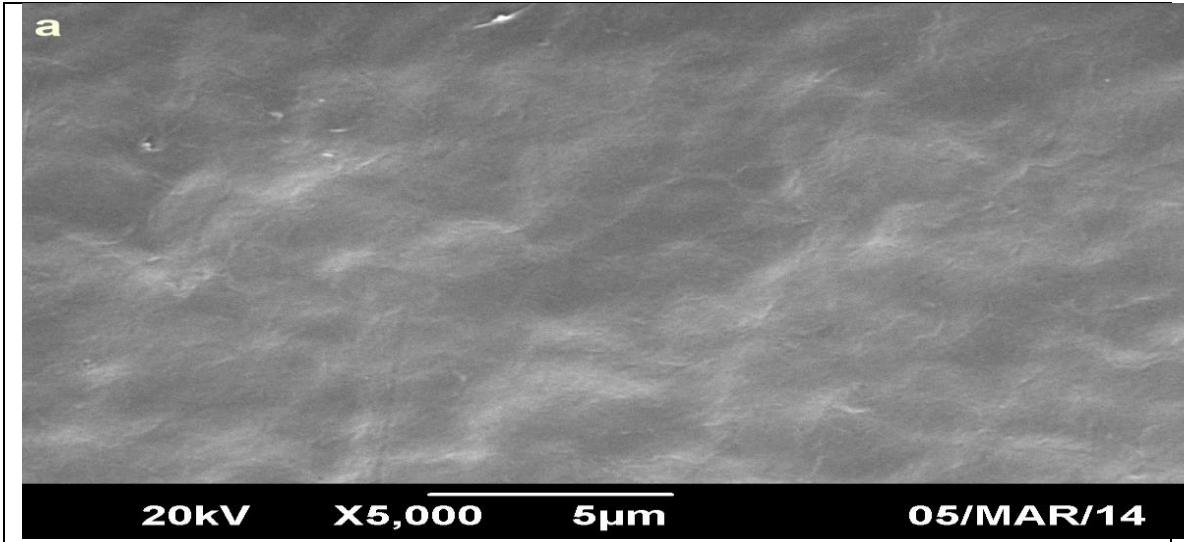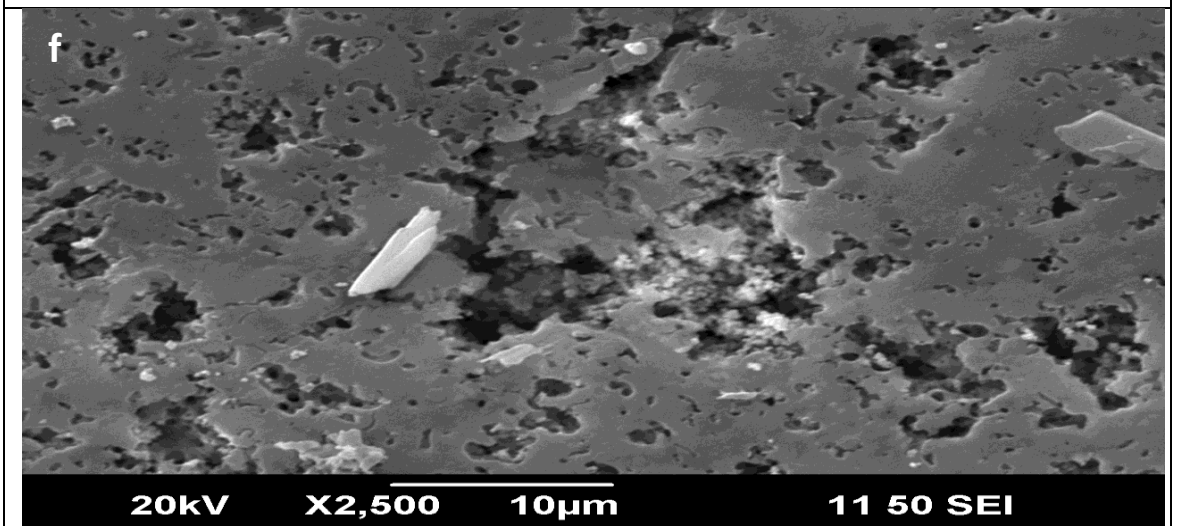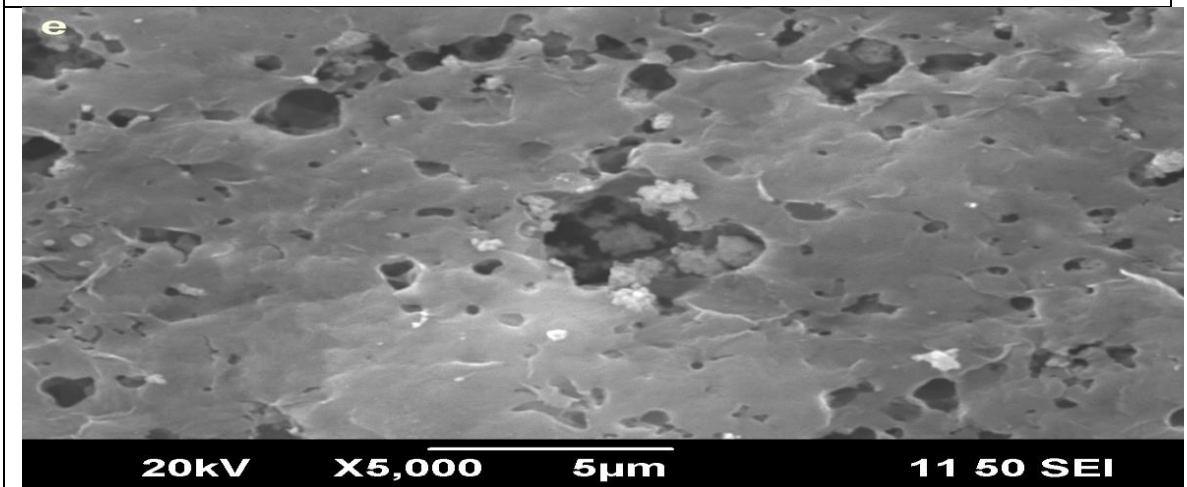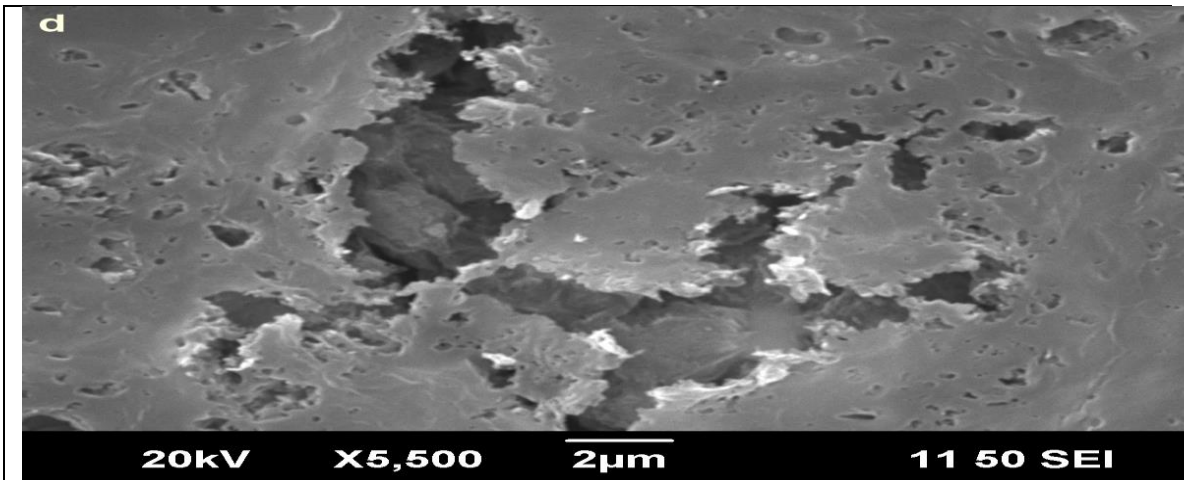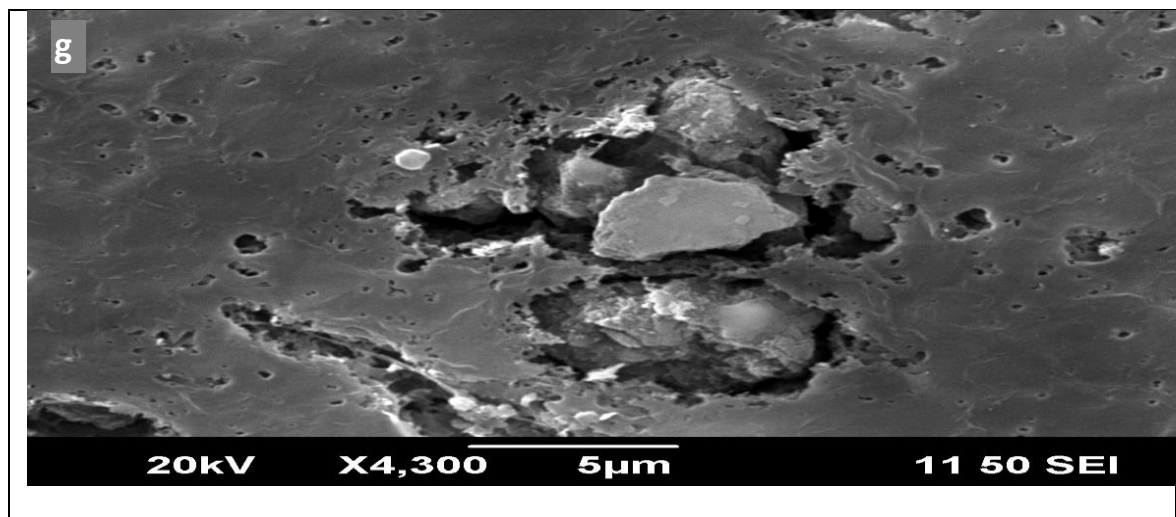
Fig 4.18. SEM images of LDPE and other composite films (a) LDPE films visible light irradiated for 45 days (b) LDPE–NPs films visible light irradiated for 45 days (c) LDPE-BG-NPs films visible light irradiated for 45 days (d) LDPE–TNPs films UV light irradiated for 15 days e) LDPE-TNTs films visible light irradiated for 45 days f) LDPE-BG-TNTs films visible light irradiated for 45 days g) LDPE-TNTs films UV light irradiated for 15 days

Figure 4.18 (d & g) show the texture of LDPE (2 wt %) composite films that were UV irradiated for 15 days. After 15 days irradiation, the surfaces of the composite film were almost completely decomposed. Hence, SEM images suggested that the degradation of LDPE matrix started from LDPE-TiO_2 interface and led to the formation of cavities around TNTs tubes aggregates. More degradation was observed under UV light by using 10% Titania nanotubes.

4.8 Surface Roughness Measurement

Contact profilometry provided 2D measurements of surface roughness of micrometer order. The test samples were PE composite films of 3 x 3 cm in area and 0.024 mm thick. Contact profilometry of PE and composite films quantify the morphology of fractures and surface irregularities in their surfaces before and after irradiation. For a given test line, the roughness was measured in micrometer as the arithmetical mean of peaks above and under the baseline (Chappard *et al.*, 2003). The mean roughness (R_a) were calculated by several samples according to ISO 8247 and their

roughness is as tabulated in Table 4.8. Maximum change in roughness was observed in 10% dye sensitized TNTs composite films. Films were smooth and plane before degradation but photo induced weight loss caused fractures and holes in films due to which surface roughness increased. There was no considerable surface roughness change in pure LDPE films before and after degradation.

Table 4.8 Surface Roughness values for pure and composite films before and after irradiation

LDPE films Composition	% Surface Roughness (R_a)		
	Before	After Visible (After 45 Days)	After UV (15 Days)
LDPE	0.526	0.67	0.71
LDPE+2% TNPs	0.645	0.88	0.99
LDPE+10%BG-TNPs	1.04	1.68	2.14
LDPE+2%TNTs	0.567	1.22	1.42
LDPE+10%TNTs	0.937	1.98	2.34
LDPE+10%BG-TNTs	1.05	1.54	2.83

4.9 FT-IR Spectrum

FT-IR spectra were used to examine the photo-catalytic degradation of films. Measurement range was $4000 - 450$ cm^{-1}. It was observed that pure PE films showed characteristics peaks in the region of 1460 cm^{-1}, 2919 cm^{-1}, 2857 cm^{-1} and 719 cm^{-1} (corresponds to CH_2 stretching and bending vibrations) which are same in all films showing that irradiation exposure do not changes the chemical properties of PE films. The spectra of composite PE films showed new peaks after irradiation around 1713cm^{-1} and 1178 cm^{-1} which could be due to absorbtions of carbonyl groups (C=O) and C–O stretching vibrations, respectively (Asghar *et al.,* 2010; Zhao *et al.,* 2006; Thomas *et al.,* 2013). FTIR spectra of different composite films are shown in Figures 4.19 to 4.23.
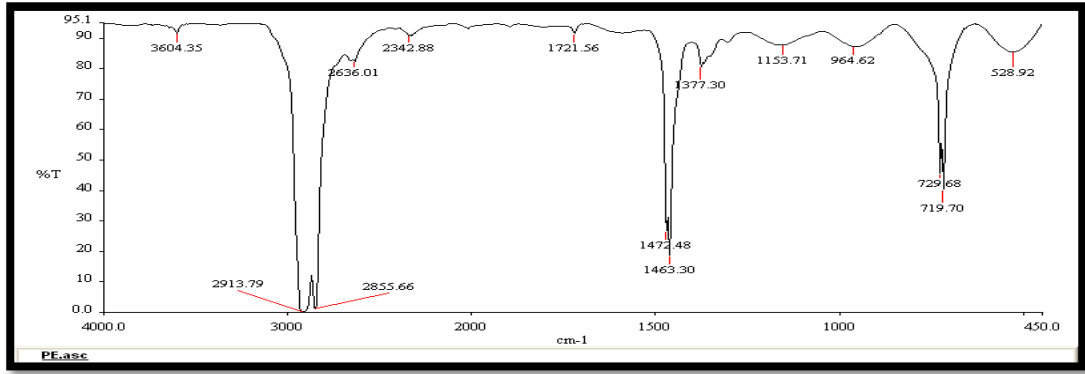
Fig 4.19 Pure LDPE films FTIR spectra before irradiation
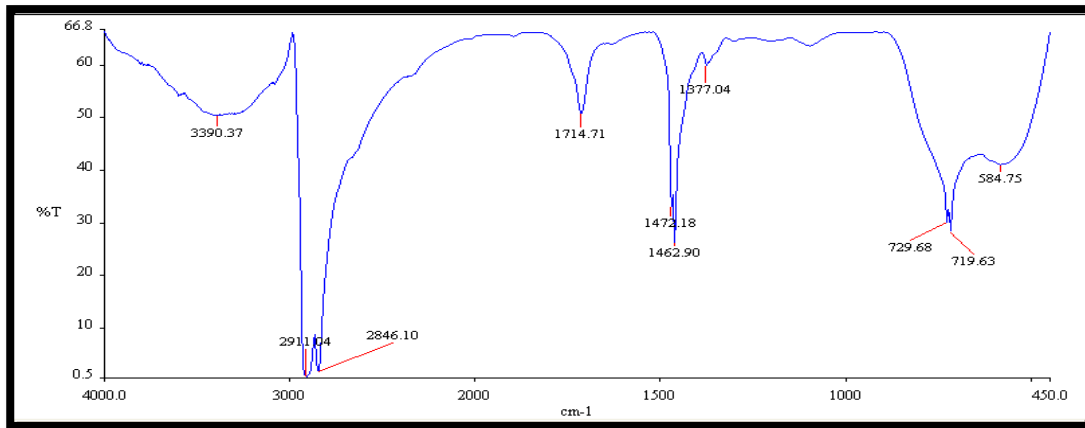
Fig 4.20 LDPE-2% TNPs composite films FTIR spectra after irradiation
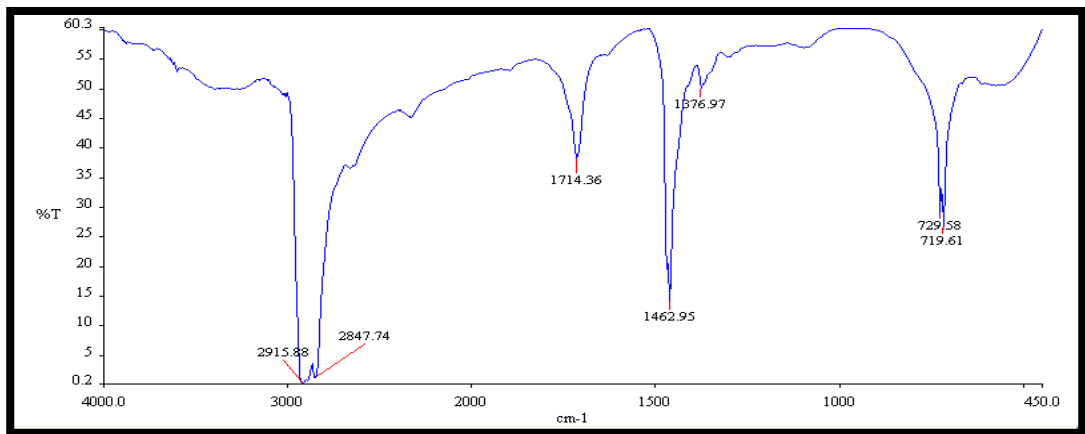
Fig 4.21 LDPE-2% BG-TNPs composite films FTIR spectra after irradiation
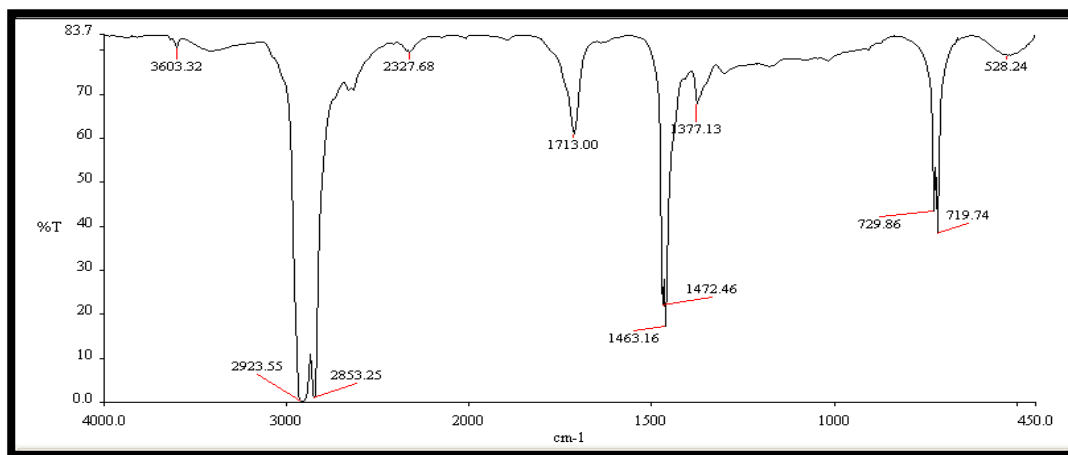
Fig 4.22 LDPE-7% TNPs composite films FTIR spectra after UV irradiation

-OH stretching region of hydroxylic group 3100-3600 showed increment in the pretreated films as highlighted in Figure 4.26. It has been reported earlier that an increase in the -OH stretching region of hydroxylic group 3050-3570 is due to formation of hydroxyperoxide and alcohol during photo-oxidation (Ibiene *et al.,* 2014). These alterations in spectra proved the structural alterations in PE films while degrading. These all spectrums indicate that the TNTs can make the photodegradation of PE film and more TNTs has a higher catalytic activity.
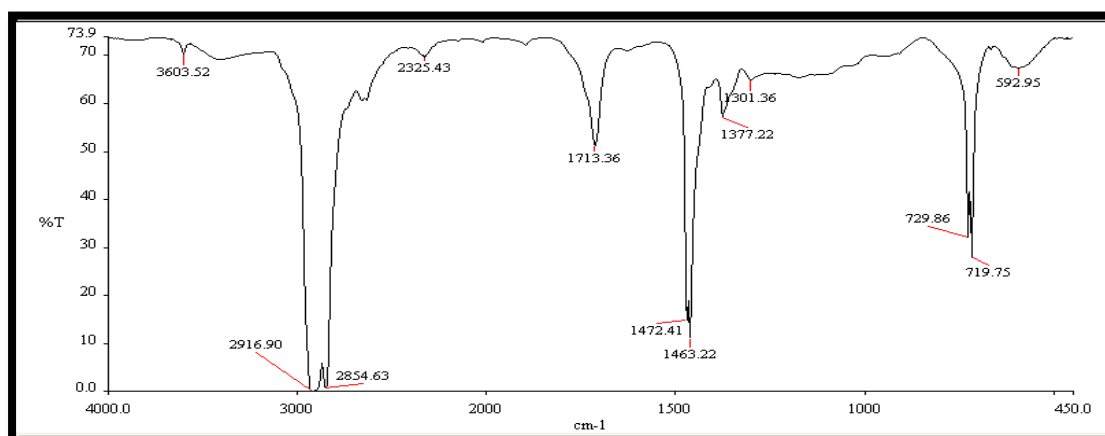
Fig 4.23 LDPE-2% TNTs composite films FTIR spectra after visible irradiation
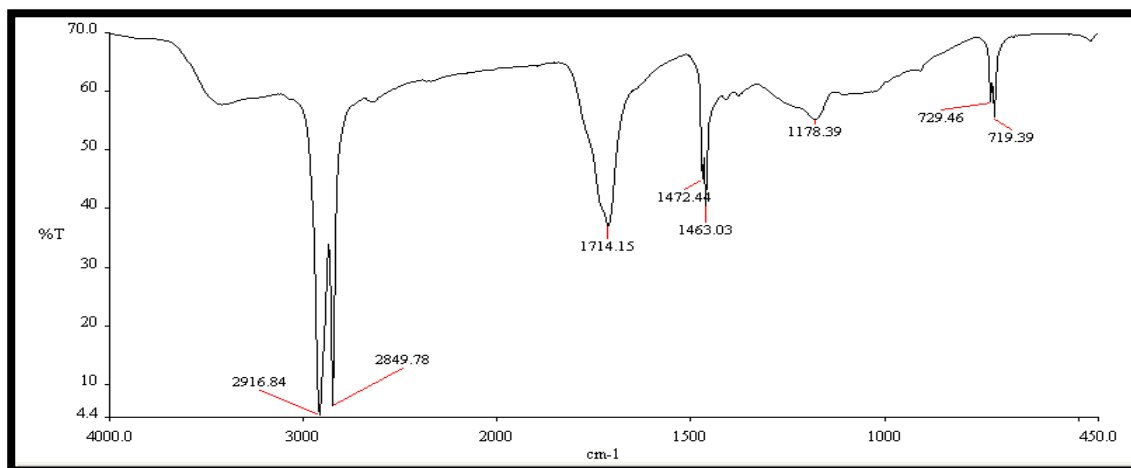
Fig 4.24 LDPE-2% BG-TNTs composite films FTIR spectra after visible light irradiation
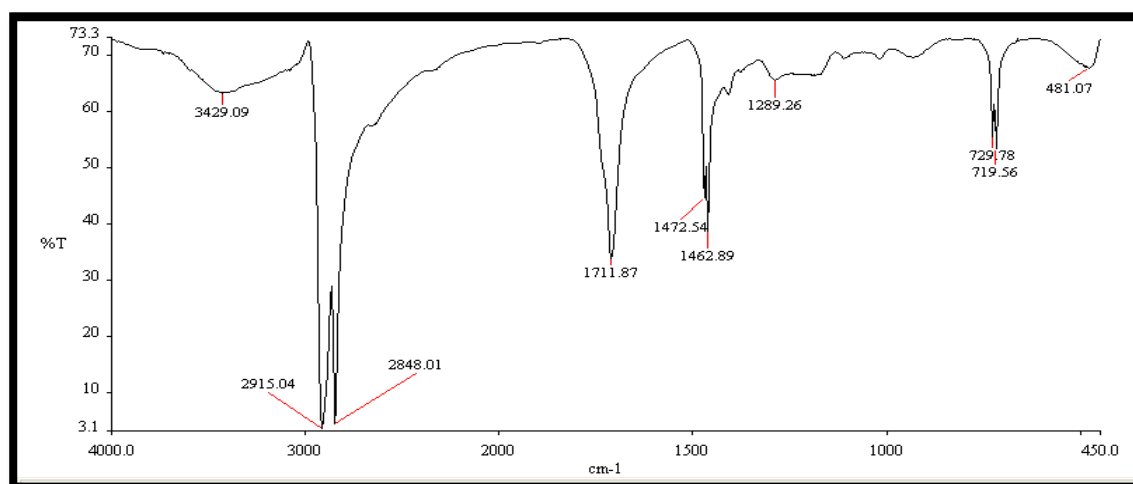
Fig 4.25 LDPE-7%TNTs composite films FTIR spectra after UV irradiation

4.9.1 Carbonyl index method for measuring quantitative effects of degradation

To quantify the degree of photo-oxidation in polyethylene films, carbonyl index is used as a measuring index which is a ratio of absorbance of carbonyl group around 1710 cm^{-1} to an internal thickness band as reference peak at 1380 cm^{-1} (Salem, 2001; Roy *et al.,* 2007).

$$\text{Carbonyl index (C.I)} = A_{1710}/A_{1380}$$

Table 4.9. Shows the carbonyl index of the LDPE and different composite films, showing increase after irradiation.

73

Table 4.9. Carbonyl Index of pure LDPE and Composite films after irradiation

Films Composition	Carbonyl index [C=O : CH$_2$]
LDPE	0.33
2%TNPs after Vis	1.2
2% BG TNPs after Vis	1.25
2% TNPs after UV	1.48
2%TNTs after Vis	1.39
2% BGTNTs after Vis	1.52
2%TNTs after UV	2.00
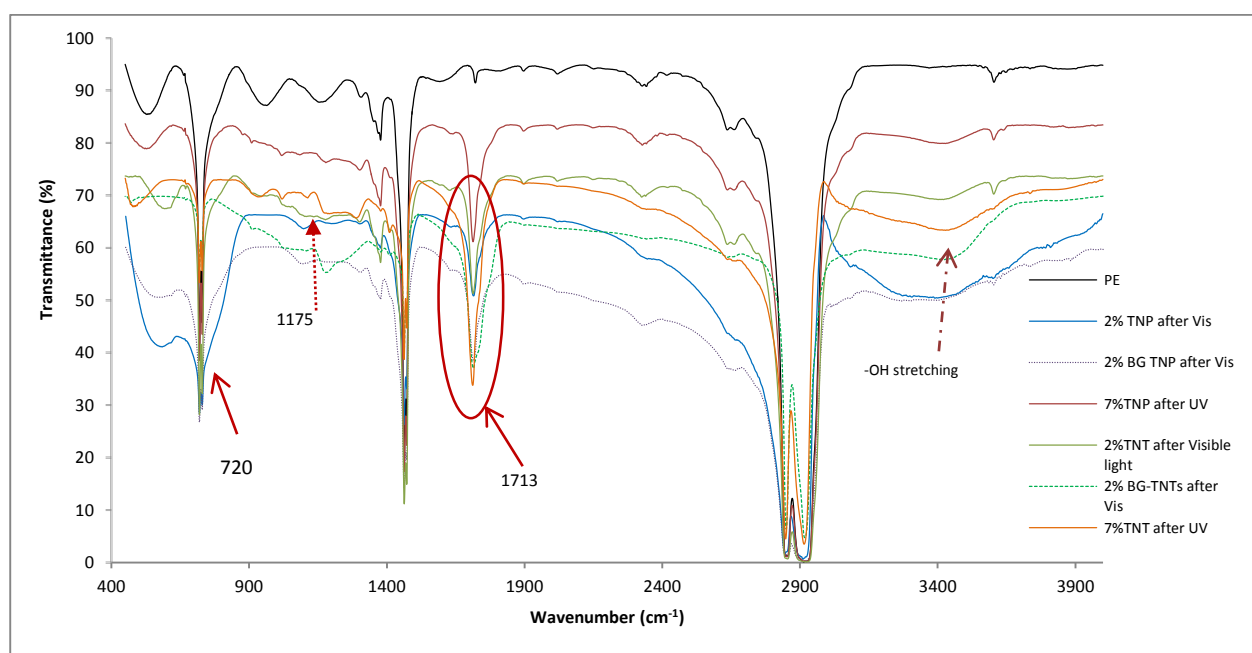
Fig 4.26 Comparison between FTIR spectra of different LDPE composite films after irradiation

The carbonyl index for PE composites which contain TNTs is higher than TNPs composites. Also TNTs enhances carbonyl index from 0.33 to maximum of 2.1 under UV light.

CONCLUSIONS AND RECOMMENDATIONS

5.1. Conclusions

This study demonstrates that

- Nanotubes were more effective than nanoparticles in photocatalytic degradation process of LDPE films

- Dye sensitization of nanostructures has increased the degradation rate of LDPE films under visible light and such films are likely to degrade under sunlight at a good rate.

- Degradation rate can be further enhanced by increasing the amount of Titania Nanoparticles or Nanotubes in the composite Films.

- LDPE-TNTs composite developed in this study will be an environmental friendly polymer material that has considerable potential for production of photodegradable shopping bags which can degrade in the open environment.

5.2 Recommendations for Future Work

In view of the results reported in this study, given below are some suggestions for future experimentation:

- At IESE degradation of Polyethylene has been investigated. It would be interesting to apply the same degradation technique to the other types of polymers like Polypropylene, polyethylene terephthalate (PET) and Polyvinyl chloride (PVC)

- Only pure titania nanotubes were studied in this work. Doped nanotubes with various metals can be used for getting enhanced degradation results

- Other titania nanostructure such as nanoribbons, nanoflowers and nanorods can be synthesized for various type of polymers degradation

- Such sort of nanocomposite LDPE bags can be introduced in market and their feasibility study can be performed

6. REFERENCES

Abou El-Nour, K. M., Eftaiha, A., Al-Warthan, A., & Ammar, R. A. (2010). Synthesis and applications of silver nanoparticles. Arabian journal of chemistry., 3(3): 135-140.

Akarsu, M., ASİLTÜRK, M., Sayilkan, F., Kiraz, N., Arpaç, E., & Sayilkan., H. (2006). A novel approach to the hydrothermal synthesis of anatase titania nanoparticles and the photocatalytic degradation of Rhodamine B. Turkish Journal of Chemistry., 30(3): 333-343.

Al-Salem, S. M., Lettieri, P., & Baeyens, J. (2009). Recycling and recovery routes of plastic solid waste (PSW): A review. Waste management., 29(10): 2625-2643.

Asapu, R., Palla, V. M., Wang, B., Guo, Z., Sadu, R. and Chen, D.H. (2011). Phosphorus-doped titania nanotubes with enhanced photocatalytic activity. Journal of Photochemistry and Photobiology A. Chemistry., 225(1): 81-87.

Asghar, W., Qazi, I. A., Ilyas, H., Khan, A. A., Awan, M. A., & Aslam, M. R. (2011). Comparative solid phase photocatalytic degradation of polythene films with doped and undoped TiO_2 nanoparticles. Journal of Nanomaterials, 2011, 12.

Authier, A. (2001). Dynamical theory of X-ray diffraction. Springer Netherlands. (534-551).

Aylward, B. Kurek, J.A, Todtenhagen, K. 1999. Polyethylene, Term Project. Retrieved from http://www.eng.buffalo.edu/courses/ce435/Polyethylene/ce435_proj.htm

Behnajady, M.A., N. Modirshahla, M. Shokri, B. Rad (2008). Enhancement of photo catalytic activity of TiO_2 nanoparticles by silver doping: Photo Deposition versus Liquid Impregnation Methods. Global NEST Journal, 10: 1-7.

Bhatkhande, D. S., Pangarkar, V. G., & Beenackers, A. A. (2002). Photocatalytic degradation for environmental applications–a review. Journal of Chemical Technology and Biotechnology, 77(1): 102-116.

Bonhomme, S., Cuer, A., Delort, A. M., Lemaire, J., Sancelme, M., & Scott, G. (2003). Environmental biodegradation of polyethylene. Polymer Degradation and Stability, 81(3): 441-452.

Braslavsky, S. E. (2007). Glossary of terms used in photochemistry, (IUPAC Recommendations 2006). Pure and Applied Chemistry, 79(3): 293-465.

Briassoulis, D., Aristopoulou, A., Bonora, M., & Verlodt, I. (2004). Degradation characterisation of agricultural low-density polyethylene films. Biosystems engineering, 88(2): 131-143.

Brunatova, T., Popelkova, D., Wan, W., Oleynikov, P., Danis, S., Zou, X., & Kuzel, R. (2014). Study of titanate nanotubes by X-ray and electron diffraction and electron microscopy. Materials Characterization, 87: 166-171.

Brunauer, S., Emmett, P. H. & Teller, E. (1938) Adsorption of gases in multimolecular layers. J. Am. Chem. Soc. 60, pp. 309-319

Butail, G., Ganesan, P. G., Teki, R., Mahima, R., & Ramanath, G. (2012). Dye-sensitized solar cells using branched titania nanotube films. Thin Solid Films, 520(7): 2764-2768.

Chakrabarti, S., Chaudhuri, B., Bhattacharjee, S., Das, P., & Dutta, B. K. (2008). Degradation mechanism and kinetic model for photocatalytic oxidation of PVC–ZnO composite film in presence of a sensitizing dye and UV radiation. Journal of hazardous materials, 154(1): 230-236.

Chanda, M., & Roy, S. K. (2012). Plastics technology handbook (Vol. 72). CRC press.

Chappard, D., Degasne, I., Hure, G., Legrand, E., Audran, M., & Basle, M. F. (2003). Image analysis measurements of roughness by texture and fractal analysis correlate with contact profilometry. Biomaterials., 24(8): 1399-1407.

Chatterjee, D., & Mahata, A. (2001). Demineralization of organic pollutants on the dye modified TiO2 semiconductor particulate system using visible light. Applied Catalysis B: Environmental., 33(2): 119-125.

Chatterjee, D., & Mahata, A. (2004). Evidence of superoxide radical formation in the photodegradation of pesticide on the dye modified TiO_2 surface using visible light. Journal of Photochemistry and Photobiology A: Chemistry., 165(1): 19-23.

Chatterjee, D., Dasgupta, S., & N Rao, N. (2006). Visible light assisted photodegradation of halocarbons on the dye modified TiO2 surface using visible light. Solar energy materials and solar cells., 90(7): 1013-1020.

Chatterjee, S. Roy, P. Surekha, P. Rajagopal, C. Choudhary, V. (2007). Studies on the photo-oxidative degradation of LDPE films in the presence of oxidised polyethylene. Polymer Degradation and Stability., 92: 1151-1160.

Chen, G. Q., & Patel, M. K. (2011). Plastics derived from biological sources: present and future: a technical and environmental review. Chemical reviews., 112(4): 2082-2099.

Chen, X., & Mao, S. S. (2007). Titanium dioxide nanomaterials: synthesis, properties, modifications, and applications. Chemical reviews., 107(7): 2891-2959.

Chiellini, E., Corti, A., & Swift, G. (2003). Biodegradation of thermally-oxidized, fragmented low-density polyethylenes. Polymer Degradation and Stability., 81(2): 341-351.

Cho, S., & Choi, W. (2001). Solid-phase photocatalytic degradation of PVC–TiO_2 polymer composites. Journal of Photochemistry and Photobiology A: Chemistry., 143(2): 221-228.

Choi, Y. E., Kwak, J. W., & Park, J. W. (2010). Nanotechnology for early cancer detection. Sensors., 10(1): 428-455.

Chowdhury, P., Moreira, J., Gomaa, H., & Ray, A. K. (2012). Visible-solar-light-driven photocatalytic degradation of phenol with dye-sensitized TiO_2: parametric and kinetic study. Industrial & Engineering Chemistry Research., 51(12): 4523-4532.

Demirors, M. (2011). The History of Polyethylene, 100+ Years of Plastics. Leo Baekeland and Beyond., 115-145

Derraik, J. G. (2002). The pollution of the marine environment by plastic debris: a review. Marine pollution bulletin., 44(9): 842-852.

Dilara, P. A., & Briassoulis, D. (1998). Standard testing methods for mechanical properties and degradation of low density polyethylene (LDPE) films used as greenhouse covering materials: a critical evaluation. Polymer testing., 17(8): 549-585.

Dogan, A. U., Dogan, M., Onal, M., Sarikaya, Y., Aburub, A., & Wurster, D. E. (2006). Baseline studies of the clay minerals society source clays: specific surface area by the Brunauer Emmett Teller (BET) method. Clays and clay minerals., 54(1): 62-66.

Ellis, S., Kantner, S., Saab, A., Watson, M., & Kadonaga, L. (2005). Plastic grocery bags: the ecological footprint. Student publications, VIPIRG publications, University of Victoria, PO Box, 3050, 1-19.

Essers, E. (2003). U.S. Patent No. 6,590,210. Washington, DC: U.S. Patent and Trademark Office.

Ezumi, M., & Todokoro, H. (1999). U.S. Patent No. 5,872,358. Washington, DC: U.S. Patent and Trademark Office.

Fa, W., Yang, C., Gong, C., Peng, T., & Zan, L. (2010). Enhanced photodegradation efficiency of polyethylene TiO_2 nanocomposite film with oxidized polyethylene wax. Journal of Applied Polymer Science., 118(1): 378-384.

Fa, W., Zan, L., Gong, C., Zhong, J., & Deng, K. (2008). Solid-phase photocatalytic degradation of polystyrene with TiO_2 smodified by iron (II) phthalocyanine. Applied Catalysis B: Environmental., 79(3): 216-223.

Fen, L. B., Han, T. K., Nee, N. M., Ang, B. C., & Johan, M. R. (2011). Physico-chemical properties of titania nanotubes synthesized via hydrothermal and annealing treatment. Applied Surface Science., 258(1): 431-435.

Fontanella, S., Bonhomme, S., Koutny, M., Husarova, L., Brusson, J. M., Courdavault, J. P., & Delort, A. M. (2010). Comparison of the biodegradability of various polyethylene films containing pro-oxidant additives. Polymer Degradation and Stability., 95(6): 1011-1021.

Fröschl, T., Hörmann, U., Kubiak, P., Kučerová, G., Pfanzelt, M., Weiss, C. K., & Wohlfahrt-Mehrens, M. (2012). High surface area crystalline titanium dioxide: potential and limits in electrochemical energy storage and catalysis. Chemical Society Reviews., 41(15): 5313-5360.

Fuertes, V. C., Negre, C. F., Oviedo, M. B., Bonafé, F. P., Oliva, F. Y., & Sánchez, C. G. (2013). A theoretical study of the optical properties of nanostructured TiO_2. Journal of Physics: Condensed Matter., 25(11): 115304.

Fujishima, A., Zhang, X., & Tryk, D. A. (2008). TiO_2 photocatalysis and related surface phenomena. Surface Science Reports., 63(12): 515-582.

Gaya, U. I., & Abdullah, A. H. (2008). Heterogeneous photocatalytic degradation of organic contaminants over titanium dioxide: a review of fundamentals, progress and problems. Journal of Photochemistry and Photobiology C: Photochemistry Reviews., 9(1): 1-12.

Gilmore, C. J. (2011). X-Ray Diffraction. Solid State Characterization of Pharmaceuticals, 35-70.

Guinier, A. (1994). X-ray diffraction in crystals, imperfect crystals, and amorphous bodies. Courier Dover Publications.

Gulmine, J. V., Janissek, P. R., Heise, H. M., & Akcelrud, L. (2002). Polyethylene characterization by FTIR. Polymer Testing., 21(5): 557-563.

Gupta, S. M., & Tripathi, M. (2011). A review of TiO_2 nanoparticles. Chinese Science Bulletin., 56(16): 1639-1657.

Halden, R. U. (2010). Plastics and health risks. Annual review of public health., 31: 179-194.

Hayat, K., Gondal, M. A., Khaled, M. M., & Ahmed, S. (2011). Effect of operational key parameters on photocatalytic degradation of phenol using nano nickel oxide synthesized by sol–gel method. Journal of Molecular Catalysis A: Chemical, 336(1): 64-71.

Herrmann, J. M. (2005). Heterogeneous photocatalysis: state of the art and present applications In honor of Pr. R.L. Burwell Jr. (1912–2003), Former Head of Ipatieff Laboratories, Northwestern University, Evanston (Ill). Topics in Catalysis., 34(1-4): 49-65.

Huang, K. C., & Chien, S. H. (2013). Improved visible-light-driven photocatalytic activity of rutile/titania-nanotube composites prepared by microwave-assisted hydrothermal process. Applied Catalysis B: Environmental.,140: 283-288.

Ibiene, A. A., Stanley, H. O., & Immanuel, O. M. (2014). Biodegradation of polyethylene by bacillus sp. indigenous to the niger delta mangrove swamp. Nigerian Journal of Biotechnology., 26(1): 68-78.

Jancar, J. (1999). Structure-property relationships in thermoplastic matrices. In Mineral Fillers in Thermoplastics I. Springer Berlin Heidelberg., (pp. 1-65).

Khan, S., Qazi, I. A., Hashmi, I., Ali Awan, M., & Zaidi, N. U. S. S. (2013). Synthesis of silver-doped titanium TiO_2 powder-coated surfaces and its ability to inactivate pseudomonas aeruginosa and bacillus subtilis. Journal of Nanomaterials, 2013: 8.

Kim, S. H., Kwak, S. Y., & Suzuki, T. (2006). Photocatalytic degradation of flexible PVC/TiO_2 nanohybrid as an eco-friendly alternative to the current waste landfill and dioxin-emitting incineration of post-use PVC. Polymer., 47(9): 3005-3016.

Konduri, M. K., Koteswarareddy, G., Rohini Kumar, D. B., Venkata Reddy, B., & Lakshmi Narasu, M. (2011). Effect of pro-oxidants on biodegradation of polyethylene (LDPE) by indigenous fungal isolate, Aspergillus oryzae. Journal of Applied Polymer Science., 120(6): 3536-3545.

Kumar, A. P., Depan, D., Singh Tomer, N., & Singh, R. P. (2009). Nanoscale particles for polymer degradation and stabilization—trends and future perspectives. Progress in Polymer Science., 34(6): 479-515.

Kyrikou, I., & Briassoulis, D. (2007). Biodegradation of agricultural plastic films: a critical review. Journal of Polymers and the Environment., 15(2): 125-150.

Lee, C. H., Kim, K. H., Jang, K. U., Park, S. J., & Choi, H. W. (2011). Synthesis of TiO_2 nanotube by hydrothermal method and application for dye-sensitized solar cell. Molecular Crystals and Liquid Crystals., 539(1): 125-465.

Lee, C. K., Lyu, M. D., Liu, S. S. & Chen, H. C. (2009). The synthetic parameters for the preparation of nanotubular titanate with highly photocatalytic activity. Journal of the Taiwan Institute of Chemical Engineers, 40(4), 463-470.

Lee, D. H., & Cho, N. G. (2012). Assessment of surface profile data acquired by a stylus profilometer. Measurement Science and Technology., 23(10): 105601.

Li, X., Wang, D. T., Chen, J. F., & Tao, X. (2012). Enhanced Photosensitized Degradation of Organic Pollutants under Visible Radiation by (I2) n-Encapsulated TiO_2 Films. Industrial & Engineering Chemistry Research., 51(3): 1110-1117.

Li, Z., Chen, Y., Shi, L., & Zhu, Y. (2007). Solid-phase photocatalytic degradation of polyethylene plastic under UV and solar light irradiation. Journal of Molecular Catalysis A: Chemical., 268(1): 101-106.

Liang, W., Luo, Y., Song, S., Dong, X., Yu, X. (2013). High photocatalytic degradation activity of polyethylene containing polyacrylamide grafted TiO_2, Polymer Degradation and Stability., 98(9): 1754-1761.

Liu, G. L., Zhu, D. W., Liao, S. J., Ren, L. Y., Cui, J. Z., & Zhou, W. B. (2009). Solid-phase photocatalytic degradation of polyethylene-goethite composite film under UV-light irradiation. Journal of Hazardous Materials., 172(2-3): 1424–9.

Macák, J. M., Tsuchiya, H., Ghicov, A., & Schmuki, P. (2005). Dye-sensitized anodic TiO$_2$ nanotubes. Electrochemistry Communications., 7(11): 1133-1137.

Mane, V. S., Deo Mall, I., & Chandra Srivastava, V. (2007). Kinetic and equilibrium isotherm studies for the adsorptive removal of Brilliant Green dye from aqueous solution by rice husk ash. Journal of Environmental Management., 84(4), 390-400.

Meeks, S. W., & Kudinar, R. (2002). U.S. Patent No. 6,392,749. Washington, DC: U.S. Patent and Trademark Office.

Montazer, M., & Seifollahzadeh, S. (2011). Enhanced self-cleaning, antibacterial and UV protection properties of nano TiO$_2$ treated textile through enzymatic pretreatment. Photochemistry and photobiology., 87(4): 877-883.

Mudgal, S., Lyons, L., Bain, J., (2011) Plastic Waste in the Environment – Revised Final Report for European Commission DG Environment. Bio Intelligence Service. http://www.ec.europa.eu/environment/waste/studies/pdf/plastics.pdf

Myshkin, N. K., Grigoriev, A. Y., Chizhik, S. A., Choi, K. Y., & Petrokovets, M. I. (2003). Surface roughness and texture analysis in microscale. Wear., 254(10): 1001-1009.

Nath, R. K., Zain, M. F. M., & Kadhum, A. A. H. (2012). Photocatalysis—a novel approach for solving various environmental and disinfection problems: a brief review. Journal of Applied Sciences Research., 8(8): 4147-4155.

Ngo, P. D. (1999). Energy Dispersive Spectroscopy. In Failure Analysis of Integrated Circuits. Springer US., (pp. 205-215).

Ni, M., Leung, M. K., Leung, D. Y., & Sumathy, K. (2007). A review and recent developments in photocatalytic water-splitting using TiO2 for hydrogen production. Renewable and Sustainable Energy Reviews., 11(3): 401-425. 37.

Njeru, J. (2006). The urban political ecology of plastic bag waste problem in Nairobi, Kenya. Geoforum., 37(6): 1046-1058.

O'Brien, T., & Thompson, R. C. (2010). Degradation of plastic carrier bags in the marine environment. Marine Pollution Bulletin., 60(12): 2279-2283.

Orhan, Y., & Büyükgüngör, H. (2000). Enhancement of biodegradability of disposable polyethylene in controlled biological soil. International Biodeterioration & Biodegradation., 45(1): 49-55.

Pan, K., Q. Zhang, Q. Wang, Z. Liu (2007). The Photo-Electrochemical Properties of Dye-Sensitized Solar Cells Made With TiO$_2$ Nanoribbons and Nanorods. Thin Solid Films., 515: 4085-4091.

Panda, A. K., Singh, R. K., & Mishra, D. K. (2010). Thermolysis of waste plastics to liquid fuel: A suitable method for plastic waste management and manufacture of

value added products—A world prospective. Renewable and Sustainable Energy Reviews., 14(1): 233-248.

Park, Y., Lee, S. H., Kang, S. O., & Choi, W. (2010). Organic dye-sensitized TiO_2 for the redox conversion of water pollutants under visible light. Chemical Communications., 46(14): 2477-2479.

Peigney, A., Laurent, C., Flahaut, E., Bacsa, R. R., & Rousset, A. (2001). Specific surface area of carbon nanotubes and bundles of carbon nanotubes.Carbon., 39(4): 507-514.

Peng, H., Li, G., & Zhang, Z. (2005). Synthesis of bundle-like structure of titania nanotubes. Materials Letters., 59(10): 1142-1145.

Poudel, B., Wang, W. Z., Dames, C., Huang, J. Y., Kunwar, S., Wang, D. Z., & Ren, Z. F. (2005). Formation of crystallized titania nanotubes and their transformation into nanowires. Nanotechnology., 16(9): 1935.

Powell, P. C., & Housz, A. I. (1998). Engineering with polymers. CRC Press.

Rajandas, H., Parimannan, S., Sathasivam, K., Ravichandran, M., & Su Yin, L. (2012). A novel FTIR-ATR spectroscopy based technique for the estimation of low-density polyethylene biodegradation. Polymer Testing., 31(8): 1094-1099.

Reazuddin, Md., (2006). Banning Polythene Shopping Bags: A Step Forward to Promoting Environmentally Sustainable Development in Bangladesh. Bangladesh Centre for Advanced Studies.

Ren, X. (2003). Biodegradable plastics: a solution or a challenge?. Journal of cleaner Production., 11(1): 27-40.

Restrepo-Flórez, J. M., Bassi, A., & Thompson, M. R. (2014). Microbial degradation and deterioration of polyethylene–A review. International Biodeterioration & Biodegradation., 88: 83-90.

Rios, L.M., Moore, C. & Jones, P.R. (2007) Persistent organic pollutants carried by synthetic polymers in the ocean environment. Marine Pollution Bulletin., 54:1230-1237.

Roy, P. K., Titus, S., Surekha, P., Tulsi, E., Deshmukh, C., & Rajagopal, C. (2008). Degradation of abiotically aged LDPE films containing pro-oxidant by bacterial consortium. Polymer Degradation and Stability., 93(10): 1917-1922.

Sadat-Shojai, M., & Bakhshandeh, G. R. (2011). Recycling of PVC wastes. Polymer Degradation and Stability., 96(4): 404-415.

Salem, M. A. (2001). Mechanical properties of UV-irradiated low-density polyethylene films formulated with carbon black and titanium dioxide. Egypt. J. Sol., 24(2): 141-150.

Savinkina, E., Kuzmicheva, G., & Obolenskaya, L. (2012). A novel titania-based photocatalyst for water purification. The International Journal of Energy and Environment., 6(2): 268-275.

Sayilkan F., Asilturk M., Sayilkan H., Onal Y. (2005). Characterization of TiO_2 Synthesized in Alcohol by a Sol-Gel Process: The Effects of Annealing Temperature and Acid Catalyst. Turkish Journal of Chemistry., 29: 697-706.

Shah, A. A., Hasan, F., Hameed, A., & Ahmed, S. (2008). Biological degradation of plastics: a comprehensive review. Biotechnology Advances., 26(3): 246-265.

Shan, A. Y., Ghazi, T. I. M., & Rashid, S. A. (2010). Immobilisation of titanium dioxide onto supporting materials in heterogeneous photocatalysis: a review. Applied Catalysis A: General., 389(1): 1-8.

Sheavly, S. B., & Register, K. M., 2007, Marine debris & plastics: environmental concerns, sources, impacts and solutions, Journal of Polymers and the Environment, 15(4), pp 301-305.

Shi, H., Magaye, R., Castranova, V., & Zhao, J. (2013). Titanium dioxide nanoparticles: a review of current toxicological data. Particle and Fibre Toxicology., 10(1): 15.

Singh, B., & Sharma, N. (2008). Mechanistic implications of plastic degradation. Polymer Degradation and Stability., 93(3): 561-584.

Stevens, E. S. (2002). Green plastics: an introduction to the new science of biodegradable plastics. Princeton University Press.

Struzhko, M. K. V., Bryksa, V. P., Murashko, A. V., & Il'in, V. G. (2011). Hydrothermal synthesis and properties of titania nanotubes doped with Fe, Ni, Zn, Cd, Mn. Semiconductor Physics, Quantum Electronics & Optoelectronics.,14(1): 21-30.

Tawashi, R., Dubuc, B., & Pimienta, C. (1994). Surface fractal dimension and the quantification of roughness of titanium implant material. Cells Mater.(USA)., 4(4): 379-386.

Tay, A. O., & Teoh, S. H. (1989). A numerical method for determining tensile stress-strain properties of plastics from total elongation measurements. Polymer Testing., 8(4): 231-248.

Teuten, E. L., Saquing, J. M., Knappe, D. R., Barlaz, M. A., Jonsson, S., Björn, A., & Takada, H. (2009). Transport and release of chemicals from plastics to the environment and to wildlife. Philosophical Transactions of the Royal Society B: Biological Sciences., 364(1526): 2027-2045.

Thomas, R. T., Nair, V., & Sandhyarani, N. (2013). TiO_2 nanoparticle assisted solid phase photocatalytic degradation of polythene film: A mechanistic investigation. Colloids and Surfaces A: Physicochemical and Engineering Aspects., 422: 1-9.

Thompson, R. C., Moore, C. J., vom Saal, F. S., & Swan, S. H. (2009). Plastics, the environment and human health: current consensus and future trends. Philosophical Transactions of the Royal Society B: Biological Sciences., 364(1526): 2153-2166.

Todokoro, H., Takami, S., Ezumi, M., Yamada, O., Ose, Y., & Kudo, T. (2003). U.S. Patent No. 6,667,476. Washington, DC: U.S. Patent and Trademark Office.

Tomás, S. A., Zelaya, O., Palomino, R., Lozada, R., García, O., Yáñez, J. M., & Ferreira da Silva, A. (2008). Optical characterization of sol gel TiO_2 monoliths doped with Brilliant Green. The European Physical Journal-Special Topics., 153(1): 255-258.

Vieyra, H., Aguilar Méndez, M. A., & Martín Martínez, S. (2013). Study of biodegradation evolution during composting of polyethylene–starch blends using scanning electron microscopy. Journal of Applied Polymer Science.,127(2): 845-853.

Vijayan, B., Dimitrijevic, N. M., Rajh, T., & Gray, K. (2010). Effect of calcination temperature on the photocatalytic reduction and oxidation processes of hydrothermally synthesized titania nanotubes. The Journal of Physical Chemistry C., 114(30): 12994-13002.

Wang, J., & Lin, Z. (2009). Dye-sensitized TiO_2 nanotube solar cells with markedly enhanced performance via rational surface engineering. Chemistry of Materials., 22(2): 579-584.

Wang, W., Varghese, O. K., Paulose, M., Grimes, C. A., Wang, Q., & Dickey, E. C. (2004). A study on the growth and structure of titania nanotubes. Journal of Materials Research., 19(02): 417-422.

Woan, K., Pyrgiotakis, G., & Sigmund, W. (2009). Photocatalytic Carbon-Nanotube–TiO_2 Composites. Advanced Materials., 21(21): 2233-2239.

Wollman, D. A., Irwin, K. D., Hilton, G. C., Dulcie, L. L., NEWBURY, D. E., & MARTINIS, J. M. (1997). High-resolution, energy-dispersive microcalorimeter spectrometer for X-ray microanalysis. Journal of Microscopy., 188(3): 196-223.

Wong, C. L., Tan, Y. N., & Mohamed, A. R. (2011). A review on the formation of titania nanotube photocatalysts by hydrothermal treatment. Journal of Environmental Management., 92(7): 1669-1680.

Xiao, Y., Wu, J., Yue, G., Xie, G., Lin, J., & Huang, M. (2010). The preparation of titania nanotubes and its application in flexible dye-sensitized solar cells. Electrochimica Acta., 55(15): 4573-4578.

Xu, X., Tang, C., Zeng, H., Zhai, T., Zhang, S., Zhao, H., Bando, Y. and Golberg, D. (2011). Structural Transformation, Photocatalytic, and Field-Emission Properties of Ridged TiO_2 Nanotubes. ACS Applied Materials and Interfaces., 3 (4): 1352–1358.

Xue, W., Zhang, G., Xu, X., Yang, X., Liu, C., & Xu, Y. (2011). Preparation of titania nanotubes doped with cerium and their photocatalytic activity for glyphosate. Chemical Engineering Journal., 167(1): 397-402.

Yoosaf, K., Ipe, B. I., Suresh, C. H., & Thomas, K. G. (2007). In situ synthesis of metal nanoparticles and selective naked-eye detection of lead ions from aqueous media. The Journal of Physical Chemistry C., 111(34): 12839-12847.

Yu, J. G., Yu, H. G., Cheng, B., Zhao, X. J., Yu, J. C., & Ho, W. K. (2003). The effect of calcination temperature on the surface microstructure and photocatalytic activity of TiO2 thin films prepared by liquid phase deposition. The Journal of Physical Chemistry B, 107(50): 13871-13879.

Yu, J., & Wang, B. (2010). Effect of calcination temperature on morphology and photoelectrochemical properties of anodized titanium dioxide nanotube arrays. Applied Catalysis B: Environmental, 94(3): 295-302.

Yu, J., Wang, W., Cheng, B., & Su, B. L. (2009). Enhancement of photocatalytic activity of mesoporous TiO_2 powders by hydrothermal surface fluorination treatment. The Journal of Physical Chemistry C., 113(16): 6743-6750.

Yu, J., Yu, H., Cheng, B., & Trapalis, C. (2006). Effects of calcination temperature on the microstructures and photocatalytic activity of titanate nanotubes. Journal of Molecular Catalysis A: Chemical., 249(1): 135-142.

Yuan, F., Li, P., & Qian, H. (2013). Photocatalytic Degradation of polyethylene glycol by nano-titanium dioxide modified with ferric acetylacetonate. Synthesis and Reactivity in Inorganic, Metal-Organic, and Nano-Metal Chemistry., 43(3): 321-324.

Yuan, Y., Ding, J., Xu, J., Deng, J., & Guo, J. (2010). TiO_2 nanoparticles co-doped with silver and nitrogen for antibacterial application. Journal of Nanoscience and Nanotechnology., 10(8): 4868-4874.

Yuan, Z. Y., & Su, B. L. (2004). Titanium oxide nanotubes, nanofibers and nanowires. Colloids and Surfaces A: Physicochemical and Engineering Aspects., 241(1): 173-183.

Zachariasen, W. H. (2004). Theory of X-ray Diffraction in Crystals. Courier Dover Publications.

Zan, L., Fa, W., & Wang, S. (2006). Novel photodegradable low-density polyethylene-TiO_2 nanocomposite film. Environmental Science & Technology, 40(5): 1681-1685.

Zhang, D., Lanier, S. M., Downing, J. A., Avent, J. L., Lum, J., & McHale, J. L. (2008). Betalain pigments for dye-sensitized solar cells. Journal of Photochemistry and Photobiology A: Chemistry., 195(1): 72-80.

Zhao, J., Chen, C., & Ma, W. (2006). Photocatalytic degradation of organic pollutants under visible light irradiation. Topics in Catalysis., 35(3-4): 269-278.

Zhao, X., Li, Z., Chen, Y., Shi, L., & Zhu, Y. (2008). Enhancement of photocatalytic degradation of polyethylene plastic with CuPc modified TiO_2 photocatalyst under solar light irradiation. Applied Surface Science., 254(6): 1825–1829.

Zhiyong, Y., Mielczarski, E., Mielczarski, J., Laub, D., Buffat, P., Klehm, U., Kiwi, J. (2007). Preparation, stabilization and characterization of TiO_2 on thin polyethylene films (LDPE). Photocatalytic applications. Water Research., 41(4): 862–74.